Geomorphology 288 (2017) 12–38

Contents lists available at ScienceDirect

Geomorphology

journal homepage: www.elsevier.com/locate/geomorph

Alluvial terrace development and changing landscape connectivity in the Great Karoo, South Africa. Insights from the Wilgerbosch River catchment, Sneeuberg

C.J. Oldknow *, J.M. Hooke

Department of Geography and Planning, School of Environmental Sciences, University of Liverpool, Liverpool, L69 7ZT, UK

ARTICLE INFO

Article history:
Received 5 December 2016
Received in revised form 7 March 2017
Accepted 10 March 2017
Available online 19 March 2017

ABSTRACT

Dendritic channel networks in the Wilgerbosch River catchment draining the south side of the Sneeuberg, South Africa, are deeply incised exposing terrace fills of varying thickness and extent. Channel long sections exhibit 'stepped' profiles where resistant rock strata cross valley floors but are now partially or completely breached. Using a combination of aerial image analysis, geomorphological mapping, sedimentological investigations (field logging, grain size, and magnetic susceptibility analyses), and geochronology (OSL, ^{14}C), this study demonstrates the patterns and controls on erosion and sedimentation and, to a lesser extent, the age structure of fills in two low-order tributaries (Africanders Kloof and Wilgerbosch Kloof) and several reaches of the higher-order Wilgerbosch River. A conceptual model of terrace development in relation to changing conditions of connectivity is presented. Valley headwaters are dominated by discontinuous palaeochannel and floodout sediments; whilst in second- to fourth-order tributaries, four sedimentologically and stratigraphically distinct terrace fills that exceed the scale and complexity of deposits on the northward side of the Sneeuberg were identified and analysed. The early part of this regional terrace succession highlights the importance of interactions between periglacial and fluvial activity on cut, fill, and pedogenesis around the time of the deglacial period. Terrace development is shown to have been a complex response to reconnection of the channel network with upland colluvial stores resulting in the valleys becoming choked with sediment. This caused a rise in groundwater and formation of extensive calcretised rootmats on valley floors and slopes acting to 'blanket' terraces 1 and 2. The thickness and longevity of this blanket is shown to restrict depth of incision in subsequent phases (T3, T4). The deposits in these headwater valleys have, until now, been overlooked as a source of palaeoenvironmental information. This study is the first to demonstrate the role and importance of changing connectivity in 'cut and fill' phases that predate the late eighteenth century European incursion in the Sneeuberg.

1. Introduction

Terraces are formed by phases of cyclic erosion and deposition (cut and fill) of alluvial sediments in a setting that generates a staircase. The causes of alluvial plain incision often reflect mixtures of external processes such as climatic, tectonic, and eustatic fluctuations (Leopold et al., 1964; Born and Ritter, 1970; Merritts et al., 1994; Bridgland and Westaway, 2008) with intrinsic factors like exceedance of geomorphic thresholds and complex response (Schumm, 1973, 1977; Patton and Schumm, 1981; Young and Nanson, 1982). Sediments generated in response to some combination of these drivers are often interbedded and can therefore render ascription of causation problematic (Erkens et al., 2009). Erosion and weathering of terrace fills can create substantive gaps in the very archives needed to reconstruct changes in river behaviour (Lewin and Macklin, 2003).

Alluvial and colluvial archives have begun to emerge as important sources of palaeoenvironmental data in South Africa, compensating for the lack of organic-based proxies; but the majority of these studies are located in the northeast of the subcontinent inside the summer-rainfall zone (Shaw et al., 1992; Botha et al., 1994; Marker, 1995; Verster and van Rooyen, 1999; Lyons et al., 2013, 2014), with a few notable exceptions (Hattingh and Rust, 1999; Holmes et al., 2003; Damm and Hagedorn, 2010; Oldknow, 2016). Several such studies have attempted to make explicit links between quantitative palaeoclimatic archives (Partridge et al., 1997) and geoproxy records with mixed success (Clarke et al., 2003; Holmes et al., 2003; Temme et al., 2008; Lyons et al., 2014). The problems with this approach include (i) extrapolation of climate records over large geographic distances; (ii) the varied response of different proxy records to the same environmental forcing (Stone, 2014); (iii) inadequate dating precision and coverage; and (iv)

* Corresponding author at: Department of Geography and Planning, Roxby Building, University of Liverpool, Liverpool, L69 7ZT, UK.
E-mail address: oldknow.cj@gmail.com (C.J. Oldknow).

http://dx.doi.org/10.1016/j.geomorph.2017.03.009

equifinality meaning that terraces may be formed under different external conditions (Soria-Jáuregui et al., 2016). Other studies in the KwaZulu-Natal, South Africa, have demonstrated the agency of autogenic drivers of landscape evolution, such as the role of geological barriers on connectivity (Tooth et al., 2002, 2004, 2007; Keen-Zebert et al., 2013) and local geomorphic thresholds controlling the age structure of colluvial deposits (Botha et al., 1994; Rienks et al., 2000).

The Sneeuberg in the Great Karoo, despite lying at an important climatic junction between summer- and winter-dominated rainfall (Chase and Meadows, 2007; Stone, 2014), is an understudied region with respect to its long-term landscape development with only a handful of Quaternary geomorphological studies in the past 30 years (Bousman et al., 1988; Holmes, 2001; Holmes et al., 2003; Boardman et al., 2005). Holmes et al. (2003), working in the Klein Seekoi River headwaters, found that the stratigraphic record lacked the scale, complexity, and age of the Masotcheni colluvium investigated by Botha et al. (1994), instead being dominated by a single phase of late Holocene incision allegedly caused by land use changes following the eighteenth century European incursion (Neville, 1996; Rowntree, 2013; Boardman, 2014). Prior to this incision, chains of pools occupied the valley floors much like those reported in Australia (Brierley and Fryirs, 1999). Grenfell et al. (2014) has subsequently proposed that these 'pools' were part of palaeo-floodout systems and that their formation was related to floodplain geomorphology. The persistence of discontinuous channels and floodouts in this and other nearby valleys was attributed to a combination of (i) reduction of upstream slope gradient by resistant dolerite sills and dikes crossing drainage lines; (ii) complex responses to do with changing valley morphodynamics; and (iii) highly episodic periods of flow (Grenfell et al., 2009, 2012, 2014).

The palaeoenvironmental significance of valley fills in the Wilgerbosch River and its tributaries (feeding the larger Sundays River) draining south of the Sneeuberg has yet to be investigated in any detail. In the last decade, research in small upland catchments here has tended to focus on reconstructing historical sediment fluxes and connectivity using a combination of gamma spectrometry and environmental magnetism (Boardman et al., 2003, 2010; Foster et al., 2007; Foster and Rowntree, 2012; Rowntree and Foster, 2012). Extensive river channel and donga (gully) incision in this area has resulted in widespread alluvial exposures revealing terrace fills of varying thickness, continuity, and pedogenic overprinting; but the processes and drivers by which they were deposited and their age structure have not been established. Channels exhibit 'stepped' profiles where resistant rock strata (dolerite, sandstone) cross valley floors, but the impact of these barriers on long-term landscape connectivity (Tooth et al., 2004; Fryirs et al., 2007; Jones et al., 2010; Fryirs, 2013) and terrace development here has not been tested.

This paper presents sedimentologic, stratigraphic, and chronologic data of terrace fills in the Wilgerbosch River catchment. We evaluate the roles of allogenic and autogenic controls on terrace development and integrate geomorphological data within existing conceptual frameworks of connectivity (Fryirs, 2013). The significance of these results are compared and contrasted with other regional geoproxy archives.

2. Regional setting

The Great Karoo is a vast (30% total land surface of South Africa) dissected landscape of plains and flat-topped mountains, characterised by east-west orientated mountain ranges, an example being the Sneeuberg in which the Sundays River originates (Fig. 1). The Sneeuberg lies within the eastern region of the Warm Temperate Zone (Sugden, 1989) at a major climatic boundary with influences from summer- and winter-dominated rains, making it a climatically sensitive region (Chase and Meadows, 2007). Annual rainfall is 423 mm·a^{-1}, concentrated in the late summer/early autumn (Grenfell et al., 2014). Diurnal and seasonal temperatures show large fluctuations: summer maxima of ca. 30 °C and winter minima of below −10 °C (Schultz, 1980).

The study area is situated just south of Compassberg (31°51′13.21″ S, 24°35′33.26″ E), the second highest peak (2502 m) in the Eastern Cape Escarpment (Boardman et al., 2003). It comprises two low-order tributaries (Wilgerbosch and Africanders Kloofs) and several reaches of the higher-order Wilgerbosch River as far as the Ganora gorge, upstream of the confluence with the Gatz River, which is a tributary of the larger Sundays River (Figs. 1 and 2).

The vegetation of the study area is characterised by 'Eastern Upper Karoo nama-Karoo (NKu 2)' on gently sloping hills, which are dominated by dwarf shrubs and 'white' grasses of the genera *Aristida* and *Eragrostis*. Thin soils, stones and boulders of steeper sandstone and slopes and dolerite ridges support dwarf karoo shrubs and drought tolerant grasses (*Aristida*, *Eragrostis*, and *Stipagrostis*) of the 'Upper Karoo Hardeveld (NKu4)' (Mucina et al., 2006).

The bedrock lithology of the area is dominated by Permian/Triassic Karoo Supergroup rocks that exhibit negligible dip (Boardman et al., 2003). Rocks of the upper Beaufort Group (Balfour and Middleton Formations) compose the sedimentary strata outcropping in these valleys. These include fining-upward sandstone-dominated sequences with mudstones, rhythmites, and sandstones with wave ripples at higher

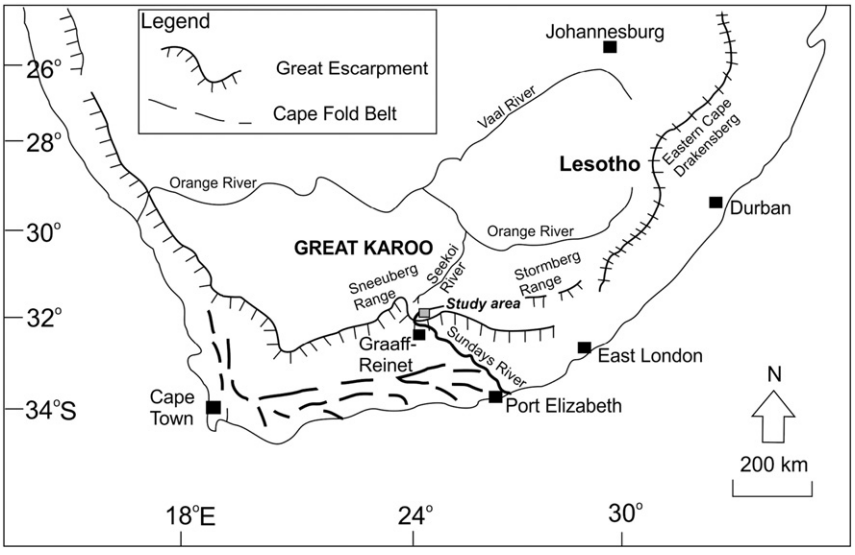

Fig. 1. Study area location in relation to Great Escarpment and other major mountain ranges and rivers of South Africa. Modified from Holmes et al. (2003).

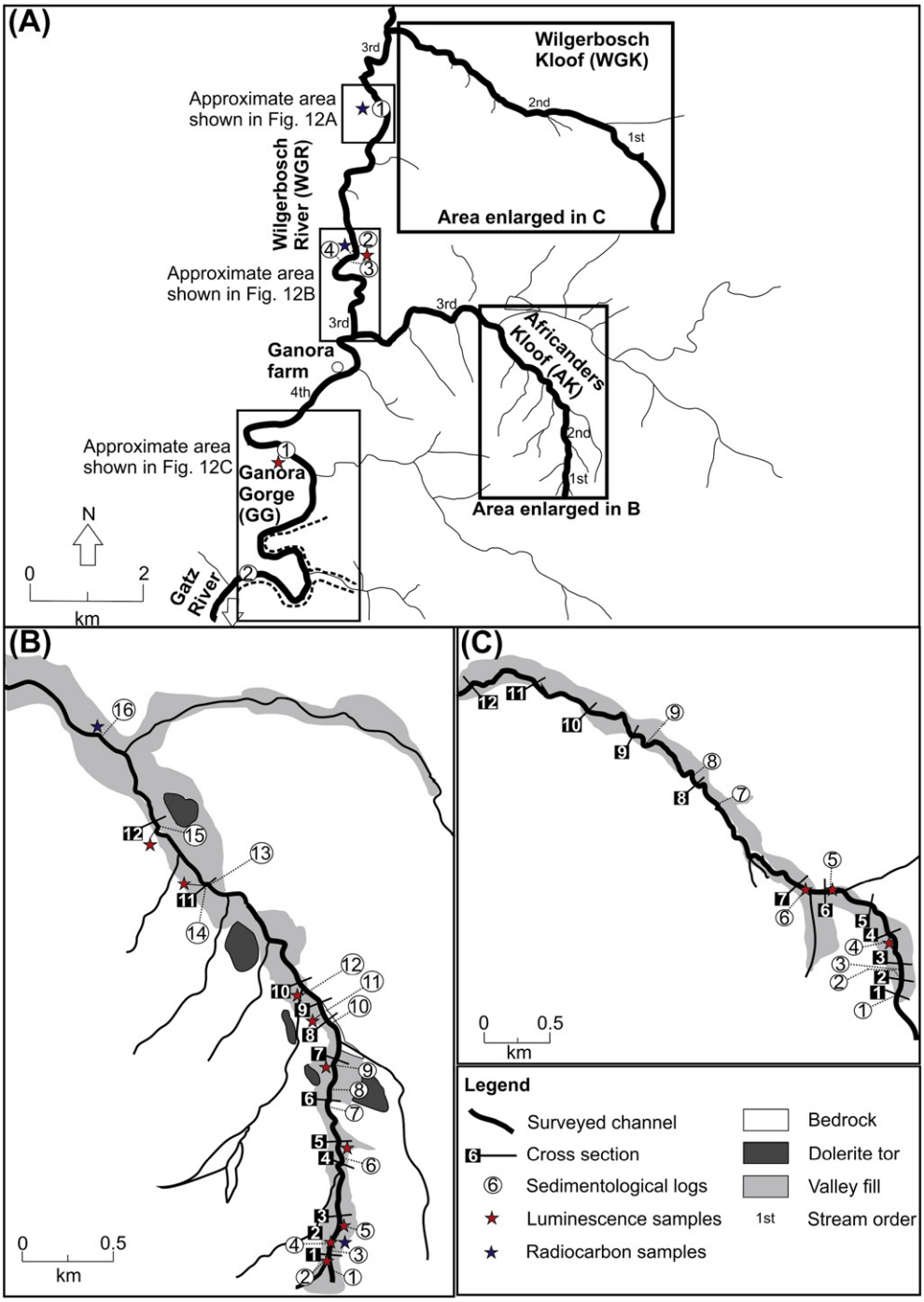

Fig. 2. (A) Map showing full extent of the study area digitised from aerial photographs. Three reaches along the Wilgerbosch River are highlighted (see Fig. 12) along with the locations of logs (Fig. 13), luminescence, and radiocarbon samples. (B) and (C) Enlarged maps of Africanders and Wilgerbosch Kloofs, respectively, showing traced limits of valley fills, location of dolerite tors, sedimentological logs (provided in Figs. 7–8 and 11), cross sections (Figs. 6 and 10), and samples collected for radiometric dating.

elevations (Turner, 1978; Cantuneanu et al., 2005). Mudstones and shales are most common on valley floors. These sedimentary rocks are extensively intruded by Drakensberg Group dolerite sills and dikes exhibiting widespread contact metamorphism (Neumann et al., 2011). Resistant sandstone beds and dolerite result in structurally controlled slopes. The relative proportions of each lithology vary between valleys. Africanders Kloof is incised into dolerite, sandstone, and mudstone to a lesser extent, whereas Wilgerbosch Kloof is carved into sandstone on the upper slopes but shale in the lower valley. The Wilgerbosch River is primarily incised through mudstone and sandstone, but dolerite sills and dikes outcrop in places.

3. Materials and methods

Continuity, elevation, morphology, and chronometric data are fundamental for correlating terrace fills laterally and longitudinally (e.g., Leopold et al., 1964; Rodnight et al., 2006; Cheetham et al., 2010). The sedimentology and stratigraphy of deposits in the Wilgerbosch catchment was investigated through aerial image analysis, extensive field reconnaissance, topographic surveys, and logging and sampling of sediment in donga and river-bank exposures.

Hartebeesthoek_1994 Datum elevations and Universal Transverse-Mercator coordinates were surveyed using a TOPCON HiPer Pro d-GPS

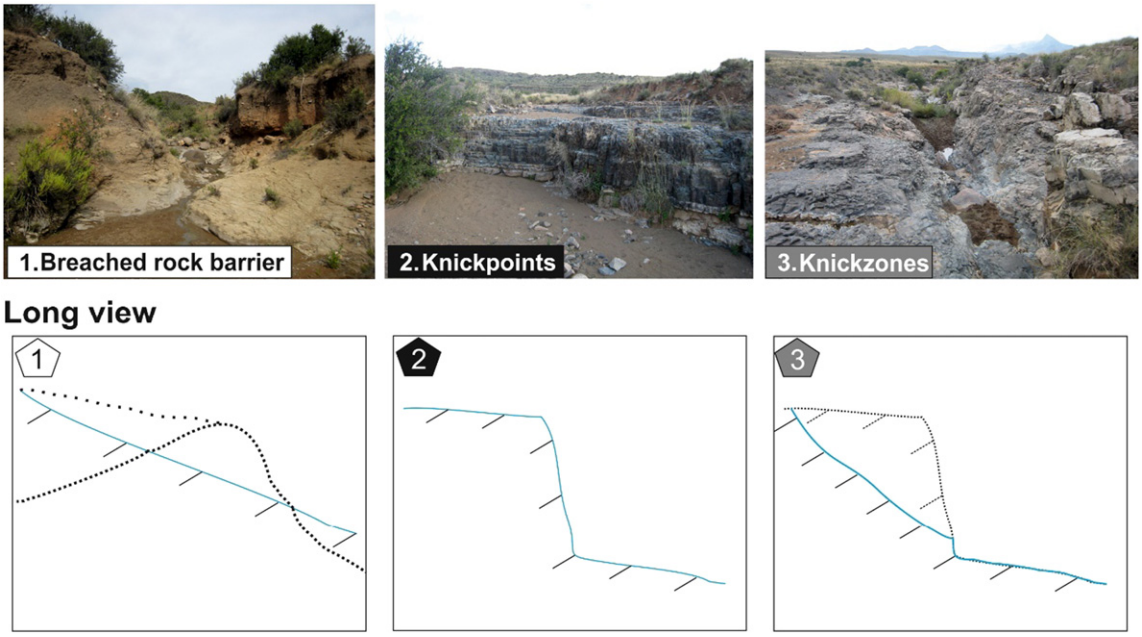

Fig. 3. Photographs and diagrams in long view of barriers classified according to degree of incision. (1) Breached rock barrier: example illustrated is a breached dolerite dike that prior to incision acted to 'dam' sediment upstream. (2) Knickpoint: the top of a zone of active incision through sandstone bedrock upstream of which the contemporary channel loses confinement and where an inset floodplain has formed. (3) Knickzones: relatively steep reaches where incision has carved an 'inner channel' into the underlying (sandstone) rock mass. Note matching symbols used in Figs. 5 and 9.

system (±2 cm accuracy) to obtain (i) channel long sections; (ii) bank top; and (iii) 24 cross sections at Africanders and Wilgerbosch Kloof. The position of possible geological barriers to sediment movement was mapped and recorded in the long profiles. Barriers were classified on the basis of morphology and extent of incision, consisting of three types: (i) breached rock barriers; (ii) knickpoints; and (iii) knickzones (Fig. 3).

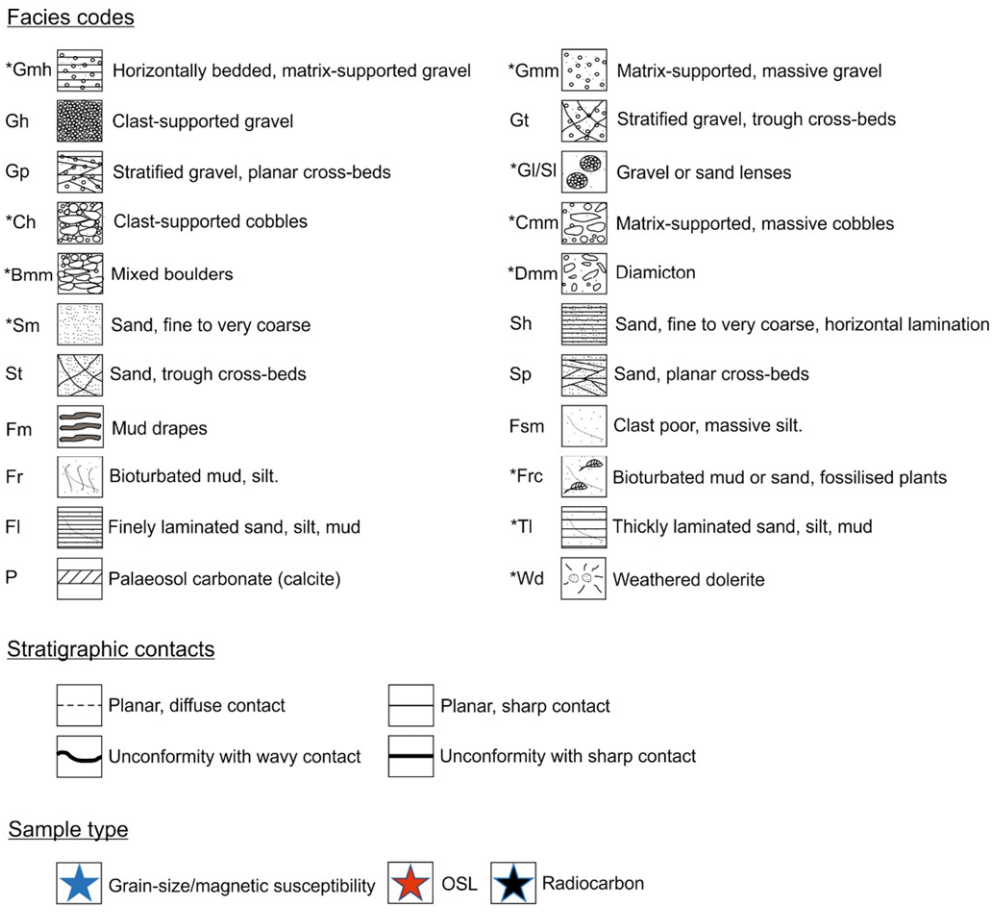

Fig. 4. Facies codes and key used in graphic sediment logs. After Miall (1996). *Additional facies codes developed to describe the valley fills in the South African field sites.

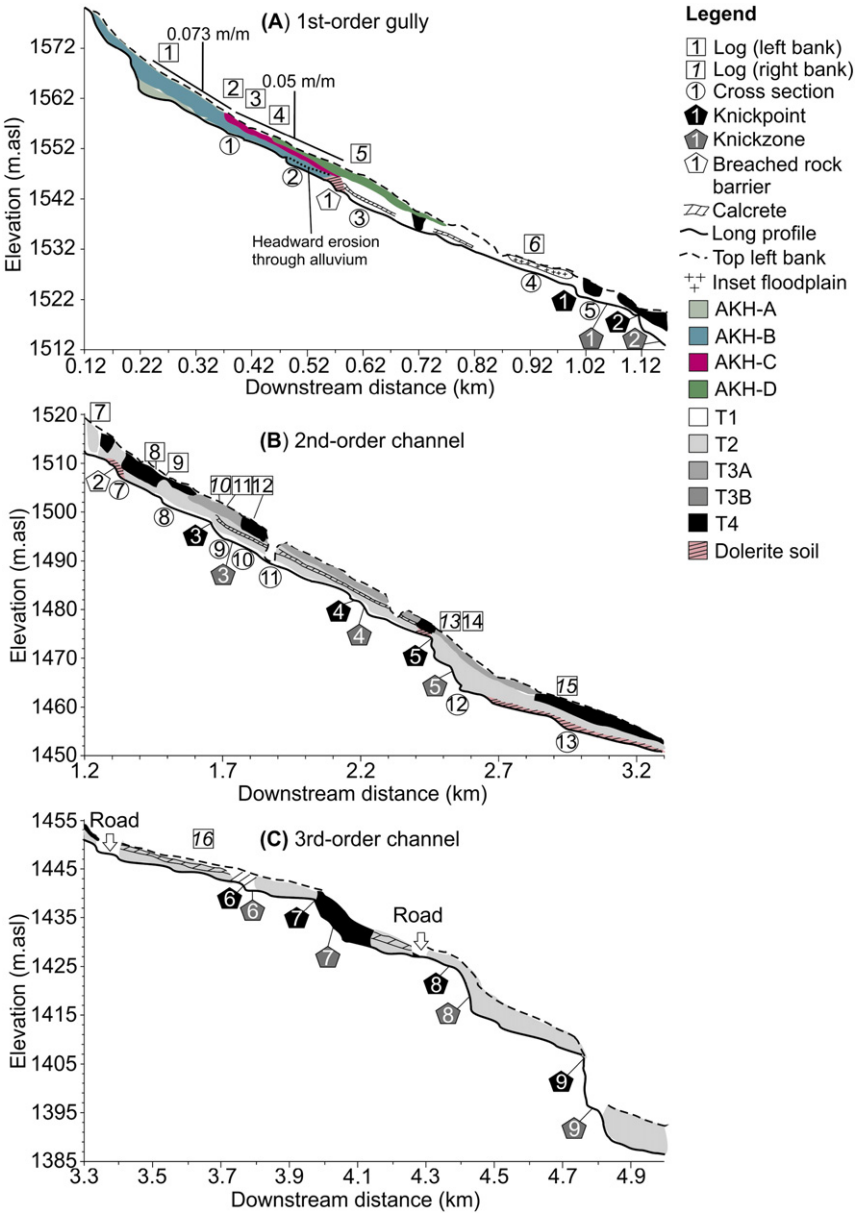

Fig. 5. Africanders Kloof long profile divided up according to: (A) first-, (B) second- and (C) third-order channels. Displayed are: (1) the longitudinal limits of valley fills in relation to channel knickpoints (black hexagon), knickzones (grey hexagon), and breached rock barriers (white hexagons); (2) locations of valley cross sections (Fig. 6); and (3) locations of sediment logs (Figs. 7 and 8).

Because of a combination of poor signal acquisition and flooding during the latter part of fieldwork along the Wilgerbosch River (including the Gorge), obtaining long profile or cross section data was not possible. Valley cross sections along the Wilgerbosch River are based upon field sketches then scaled using aerial photographic imagery.

To identify the main vertical, longitudinal, and lateral variations in slope, channel, and overbank deposits, sedimentological logs were obtained at 31 sites (Fig. 2). Sampling strategy ensured that all major deposits within reaches were represented. Elevation of logs was obtained using a handheld GMS-2 GPS system (±10 cm accuracy). Field descriptions of particle size were undertaken using grain-size analysis cards. The extent of each type deposit was either physically traced in channel-bank exposures or augered, and the limits mapped using the GMS-2. Sediment logs were constructed to show changes in facies, sedimentary structures, and stratigraphic boundaries (Fig. 4). The Udden-Wentworth scale (Wentworth, 1922) was used to classify grain size. Selected samples from major stratigraphic units were collected for laser diffraction and determination of magnetic susceptibility (X_{LF}) (Appendix A). Laser diffraction data is used to (i) characterise matrix composition (0–2 mm) in coarse deposits and (ii) total sediment distribution where sedimentary unit grain size is <2 mm. Calculation of grain-size distributions and parameters was achieved using the GRADISTAT (v.8) program (Blott and Pye, 2001). Sampling density was controlled by the need to adequately characterise major stratigraphic units within bank exposures and 'fingerprint' the various deposits.

The combined evidence of surveyed channel morphology and the limits of fills were used to produce annotated long profiles (Figs. 5 and 9) or annotated air-photos (Fig. 12) to analyse the longitudinal and lateral distribution of terraces in relation to potential barriers. Valley cross sections (Figs. 6, 10, and 14) and sediment logs (Figs. 7, 8, 11, and 13) enable the lateral limits, junctions, and nature of the facies to be visualised three-dimensionally, whilst facies descriptions and interpretations are outlined in Table 1 and Appendix A (Table A.1). Correlations between logs were based on mapped continuity of deposits, major junctions between fills, lithostratigraphy, and magnetic susceptibility and remanence parameters (Oldknow, 2016).

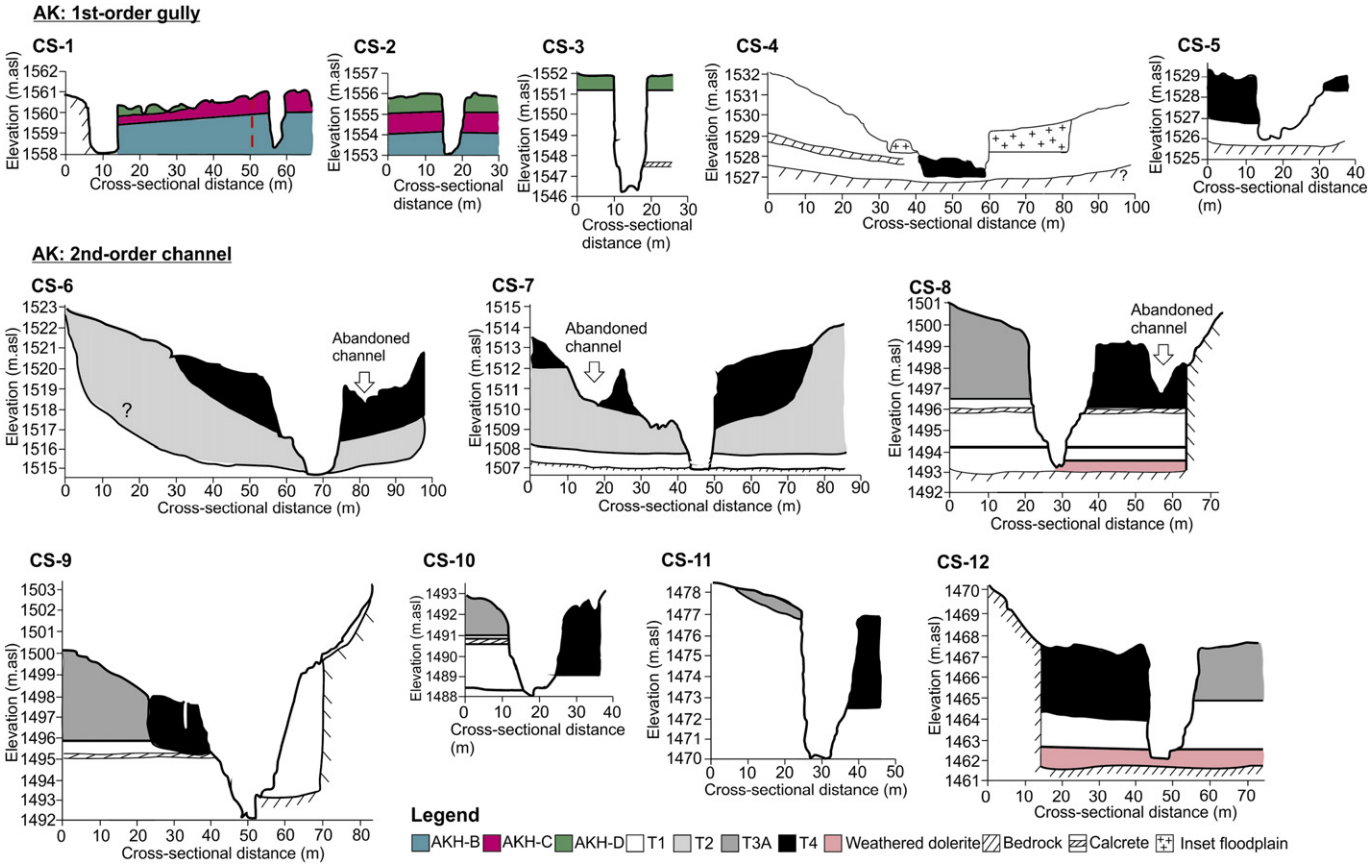

Fig. 6. Valley cross sections showing the stratigraphic relations between the terrace fills at Africanders Kloof.

Twenty-nine optically stimulated luminescence (OSL) samples were collected from 14 outcrops (Fig. 2) representing the optimum tradeoff between coverage of deposits but, where possible, avoiding unsuitable sections on the basis of (i) bioturbation; (ii) lack of homogeneous sandy units; and (iii) units <20 cm thick. Large samples (1 kg) were collected at night by cleaning sections and shovelling sediment into opaque black bags, which were then sealed tightly prior to shipment. Repeat samples from stratigraphic horizons were collected to determine moisture content and radiation dose rates.

Sample preparation for OSL analyses was performed under red-light conditions. Wet sieving was employed to remove silts and clays and to concentrate sediment in the 200–300 μm range. Samples were subjected to a series of acid and density separation protocols, including (i) 10% HCL to dissolve carbonates; (ii) 30% H_2O_2 to dissolve organic matter; (iii) density separations ($2.62 < \rho < 2.76$ g/cm^2) to concentrate quartz; and (iv) treatment of quartz-rich fraction with 40% HF acid for 45 min to dissolve remaining feldspar grains and to remove the alpha-irradiated surface (10 μm) on quartz grains. At the density separation stage, very high proportions of feldspar (>50%) were collected, necessitating use of the strong (40%) HF etch. All samples reacted strongly to the etch yielding such low quartz amounts that of the 29 samples collected only 2 could be dated. This was achieved by combining the finer grain size fractions, resulting in unconventionally large grain size windows (LV-509: 90–300 μm; LV-515: 90–200 μm; Table 2). Etched quartz grains were mounted onto the inner 1 mm of 1-cm aluminium discs using Silkospray in preparation for single aliquot measurements.

The OSL analyses were conducted on an automated Risø DA-15 B/C reader equipped with 21 blue LEDs (470Δ30 nm) for stimulation employed at 80% of full diode current providing ~17 mW·cm^{-2} power from the blue LED unit and 370 mW·cm^{-2} from the IR laser diode (830 nm). Initial measurements were made at 125 °C and were detected through a Hoya U340 filter (transmitting 320–390 nm). Aliquots were rejected on the basis of (i) low count rates (<300); (ii) recycling ratio > 10% from unity; (iii) detection of feldspar contamination (IRSL depletion ratio > 10% from unity; Duller, 2003); (iv) failure to fit exponential or exponential plus linear function to growth curve; (v) the OSL signal not exhibiting a fast component; and (vi) significant recuperation (>5%; Murray and Wintle, 2000).

Chemical analyses for determination of K, U, and Th were carried out at University of Liverpool using inductively coupled plasma mass spectrometry (ICP-MS) and inductively coupled plasma atomic emission spectrometry (ICP-AES). The conversion factors of Adamiec and Aitken (1998) were used to convert those concentrations to environmental dose rates (Gy/ka).

LV-509: A modified SAR-protocol (Murray and Wintle, 2000) that included a hot-bleach step (OSL measured at 125 °C for 40 s for the test dose) was used in both preheat/dose recovery tests and final D_e measurements to cure problems of poor low dose recycling and recuperation (Oldknow, 2016). **LV-515**: the normal SAR protocol was suitable for preheat, dose recovery, and D_e measurements. A preheat of 240 °C for 10 s along with a cutheat of 200 °C for the test dose were used in final D_e measurements for both samples. The Central Age Model (CAM) was used to calculate final burial age for both samples following the protocol of Arnold et al. (2007).

Fossilised plant remains (*Juncus* stems) for AMS radiocarbon dating were sampled from four sediment exposures to determine the alluvial chronology. Samples were prepared and analysed at the Oxford Radiocarbon Accelerator Unit, but yielded insufficient carbon; therefore, only 1 of 10 was successfully dated. The dated sample (P-37289) was calibrated using the SHCal13 atmospheric curve (Hogg et al., 2013).

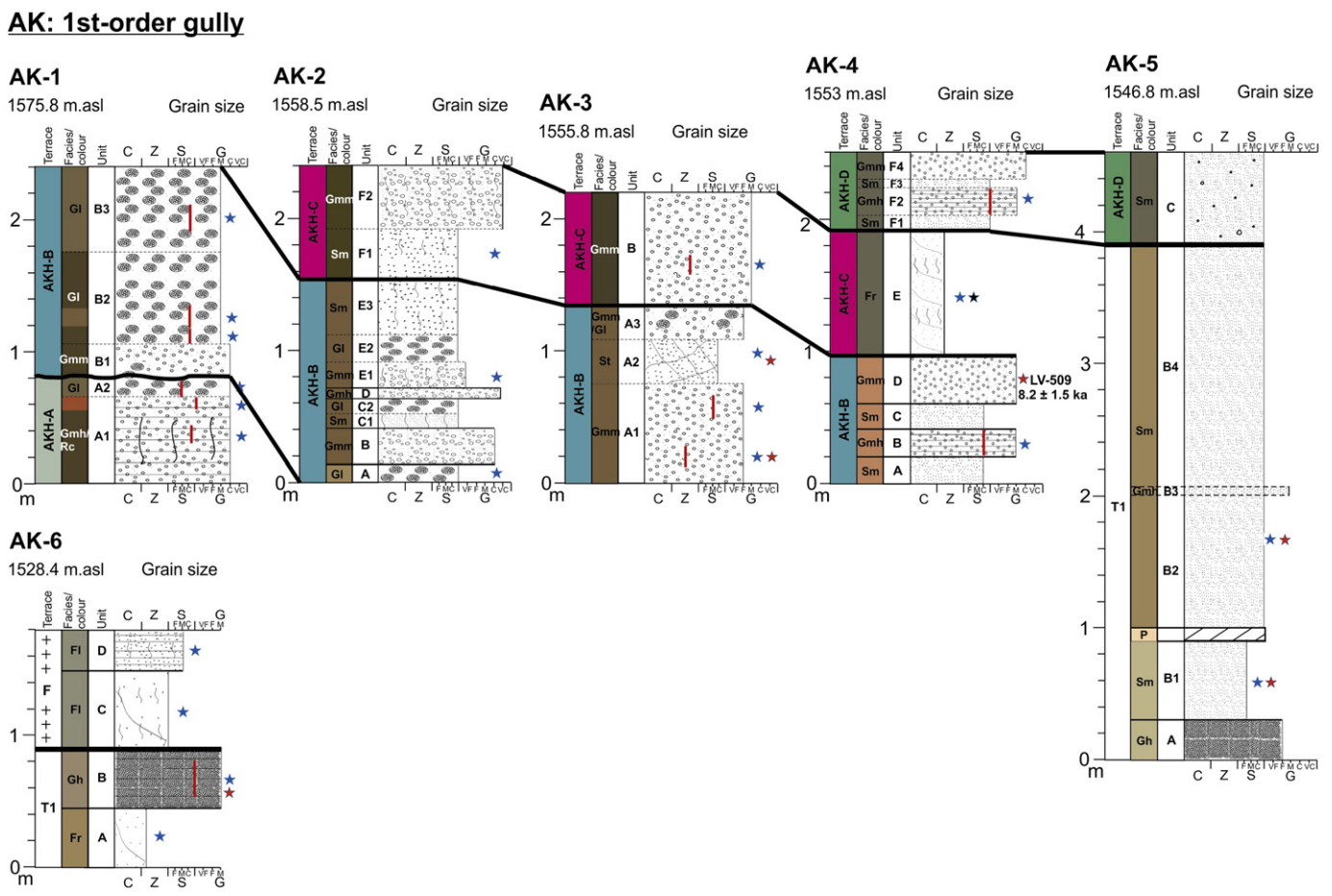

Fig. 7. The alluvial succession exposed in the first-order channel bank exposures (AK-1-6) at Africanders Kloof. Note sand/silt units are scaled according to their D_{50} grain size; red lines are used to indicate matrix D_{50} determined from Coulter measurements for coarser gravel units.

4. Results

4.1. Discontinuous valley fill development

The headwaters of both tributaries (Africanders and Wilgerbosch Kloofs; Fig. 2) contain a range of alluvial facies of varying thickness and longitudinal extent as summarised in Table 1 and outlined in the forthcoming subsections (Sections 4.1.1–4.1.3). Groups of facies typically occur together, allowing several facies associations to be defined that include deposition in confined and unconfined situations.

4.1.1. Africanders Kloof headwaters

The contemporary gully has retreated headward part way up the sandstone footslopes of a mesa capped by dolerite. The gully has exposed up to 2.5 m of alluvium, and its base is situated at or just above bedrock. Four distinct morphostratigraphic units with unconformable bed contacts were identified in gully sidewall exposures (Figs. 5A, 8; Table 1). Cross sections 1 and 2 show that units B-D dip away from the modern gully (Fig. 6). Unit AKH-A consists of up to 1.2 m of thinly bedded, matrix-supported gravels that exhibit weak or no grading. This unit terminates 0.3 km downstream. Unit AKH-B is thicker than A (up to 1.6 m), consisting of pedogenically altered matrix-supported gravels, lenticular gravels, and massive sands with sharp bedding contacts. This unit is traceable as far as breached rock barrier 1 (a deeply weathered dolerite outcrop) where it terminates (Fig. 5A). Unit AKH-C is less thick than A and B (0.95 m). It extends from 0.35 km, 50 m upstream of a reduction in slope gradient (0.05 compared to 0.073 m/m), to breached rock barrier 1. Compared to units A and B, unit C exhibits proximal to distal fining. For example, very coarse gravels at AK-2, medium gravels at AK-3 and clayey silt at AK-4 (Fig. 7). Particle size analysis indicates matrix-fining from AK-3 to 4 (D_{50}: 44–9.6 μm; Table A.2).

Unit AKH-D consists of distinctive infilled palaeogully architecture carved into unit C. Otherwise deposits consist of up to 0.6 m of bedded, unaltered coarse gravels and sand. Proximal-distal fining is evident (AK-4 and 5). Unlike the other headwater units (A-C), AKH-D extends over breached rock barrier 1 (0.45–0.9 km) burying T1 and T4 (see Section 4.2.1). Magnetic susceptibility values for each unit typically exceed 100 (Table A.2). Headward erosion of the modern gully has produced a 0.6 m knickpoint through these headwater deposits (AKH-B and C) that corresponds to the top of breached rock barrier 1 (Fig. 5A).

4.1.2. Wilgerbosch Kloof headwaters

The Wilgerbosch Kloof headwaters originate at the base of a deeply eroded mesa 2 km north of Africanders Kloof. The upper sandstone slope where the definable channel commences is very steep (0.24 m/m; Fig. 9A) but is buffered from the mesa by a pediment formed on sandstone. Two morphostratigraphic units were identified. Unit WGK-A extends from 0.11 to 0.35 km downstream (Fig. 9A). The facies consist of pedogenically altered, sharply bedded units of matrix-supported gravels, cobbles, and boulders interspersed by units of sand (Fig. 11; Table 1). These headwater deposits, unlike those in the Africanders Kloof, do not terminate abruptly at any lithological impediment. The soil overprinting the deposits was traced downstream and overprints terrace 2 (see Section 4.2.2). Unit WGK-B extends from the top of the sandstone slope to 0.3 km (Fig. 9A). The facies consist of unaltered units of sand and either massive or faintly bedded gravel. Unit thickness and grain size decline downstream (Fig. 10: CS-1-3; Fig. 11: WGK-1-3). Magnetic susceptibility values for both units are consistently lower than those at Africanders Kloof (Table A.2).

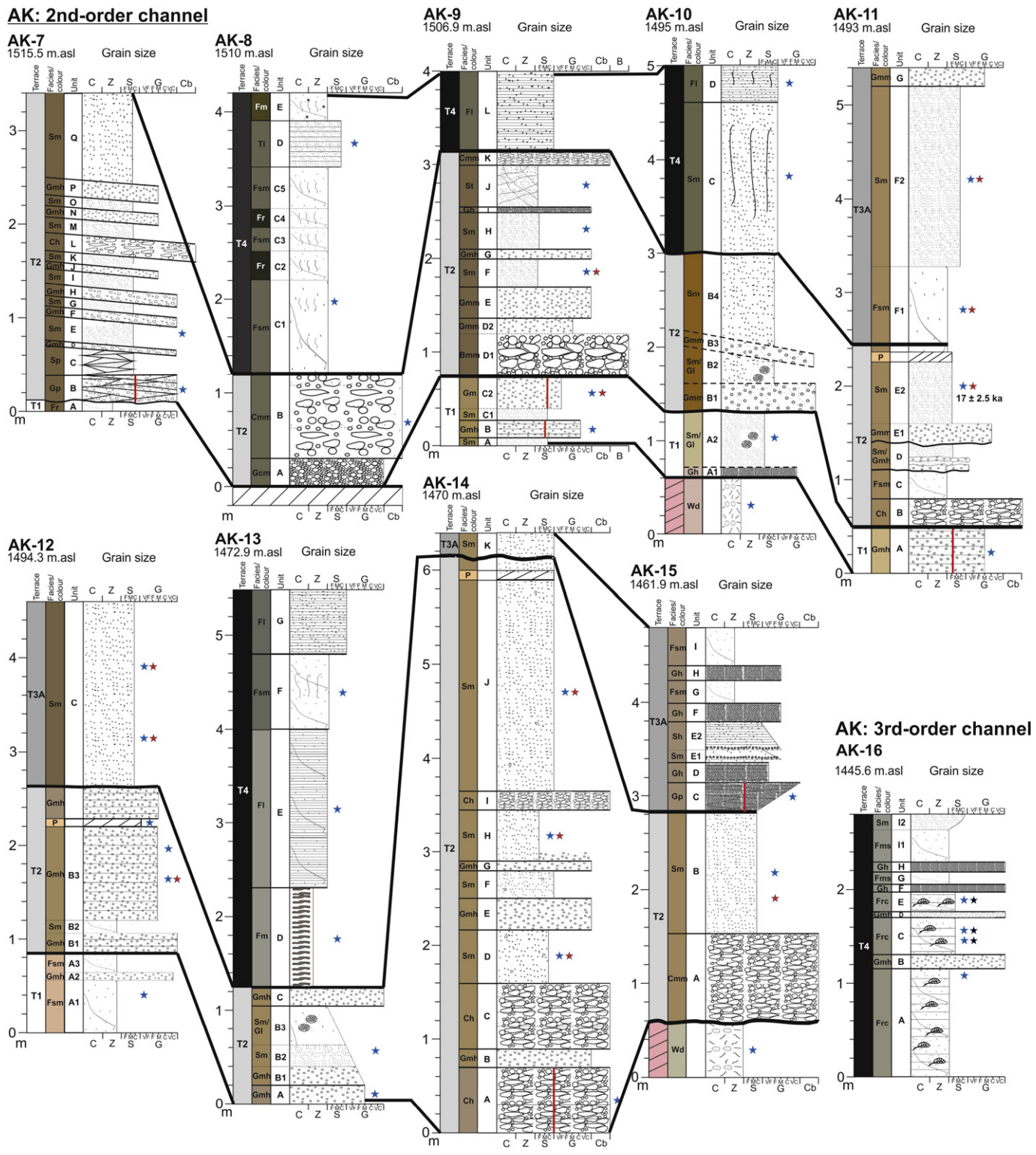

Fig. 8. The alluvial succession exposed in second- and third-order channel bank exposures (AK-7-16) at Africanders Kloof.

4.1.3. Wilgerbosch River

Fig. 13B shows several localised deposits impinging laterally on the valley floors in between the larger terraces (Section 4.2). The facies at site WGR-4 consist of very fine to fine sand (D_{50} = 66–187 μm) that are buried by 2.5 m of massive, matrix-supported sandstone and mudstone gravels (Table 1). Magnetic susceptibility is substantially lower (X_{LF} = 27–42) than valley fills in the first-order tributaries (Table A.2).

4.2. Continuous valley fill development

In the higher-order streams, up to four major terrace fills were identified, mapped, and analysed across the study region. Data on terrace extent, morphology, thickness, and sedimentology are summarised in Table A.1 (see Appendix A) and outlined in the following subsections (Sections 4.2.1–4.2.5).

Table 1
Sedimentary characteristics for headwater tributary fills; facies codes modified from Miall (1996).

Terrace	Log/unit	Summary description	Interpretation
AKH-A	AK-1/A	Altered, mottled, thinly bedded matrix-supported (Gmh) and lenticular gravels (Gl). Bed thickness: 0.07–0.1 m.	Sheet-flood deposition after transition from entrenched to unconfined channel.
AKH-B	AK-1/B AK-2/A-E AK-3/A AK-4/A-D	Altered, mottled, matrix-supported gravels (Gmm and Gmh), lenticular gravels (Gl), and massive sands (Sm). Bed thickness: 0.05–0.77 m.	Infilled floodout distributary channel and buried overbank sediments.
AKH-C	AK-2/F AK-3/B AK-4/E	Altered units of massive sand (Sm), matrix-supported gravel (Gmm and Gmh), and silty clay (Fr). Bed thickness: 0.3–1 m.	Debris flow deposits laid down in a floodout with progradational fining.
AKH-D	AK-4/F AK-5/C	Unweathered alternating sand (Sm), horizontally bedded matrix-supported gravel (Gmh) and coarser gravels with weak bedding (Gmm). Bed thickness: 0.04–0.1 m.	Infilled palaeogully and overbank sediments. Debris flow deposits mantle the surface.
WGK-A	WGK-2/A-B WGK-3/A-F	Altered, mottled units of matrix-supported gravels, cobbles and boulders. Gravel facies vary: massive (Gmm) to thinly bedded (Gmh) or exhibit planar (Gp) or trough (Gt) cross-bedding. Altered sandy units: massive or with trough cross-beds (Sm/St). Bed thickness: 0.02–0.6 m.	Alluvial fan channel deposits.
WGK-B	WGK-1/A WGK-2/C WGK-3/G	Unweathered alternating units of sand (Sm) and gravel (Gmm and Gmh); massive or with faint bedding that dips downstream. Bed thickness: 0.05–0.5 m.	Debris flow and slopewash deposits in an alluvial fan.
Unclassified	WGR-4/A-B	Altered, mottled units of fine sand (Sm) which exhibit inverse grading to massive, matrix-supported gravels (Gmm).	Debris flow and slopewash deposits in an alluvial fan.

4.2.1. Terrace 1

Terrace 1 occurs at the valley margins of Africanders Kloof (Fig. 6: CS-3-10) and two reaches of the Wilgerbosch River (Figs. 12B and C) but is absent at Wilgerbosch Kloof. At Africanders Kloof it consists of deeply weathered, massive or thin-medium horizontally bedded sands or clayey silts (see AK-5, Fig. 7) overprinted by calcrete. This calcrete was traced downstream where it also overprints terrace 2 (see Section 4.2.2 for description). Inverse grading is a common feature. Basal units typically possess a D_{50} grain size of finer than 110 μm, whilst upper units range from 130 to 1159 μm (Table A.3). Localised gravels occur in places either infilling small palaeogully structures or occurring as laterally discontinuous beds. The deposits are thickest (up to 5 m) in a bedrock depression immediately downstream of breached rock barrier 1 (Fig. 5A) behind which three discontinuous terrace units are preserved (see Section 4.1.1). In contrast to the headwater fills (AKH-A-D), the terrace surfaces dip toward rather than away from the contemporary gully (CS-3-10: Fig. 6). Additionally, X_{LF} is typically lower than the AKH units immediately upstream of breached rock barrier 1 (Tables A.2 and A.3).

Downstream of knickpoint 2 (Figs. 5B and C), T1 is deeply incised by palaeochannels such that only up to 0.8 m of the succession is preserved and, in some cases, has been stripped completely. Furthermore, the sedimentological expression of T1 deposits is subtly different to the first-order gully with increased prominence of horizontally bedded medium gravels (AK-9 and 11: Fig. 8) rather than massive fine sediments (AK-5: Fig. 7).

Along the Wilgerbosch River, T1 is most completely expressed in the Ganora Gorge, where between 4.5 and 6 m of sediment has accumulated (GG-S, GG-2: Figs. 12C and 13), though its sedimentology is markedly different from T1 deposits at Africanders Kloof. For example, the facies in the gorge include (i) diamictic sediments consisting of vertically oriented, platy gravel clasts within a poorly sorted matrix of sandy silt; and (ii) laterally discontinuous clast-supported gravels. Unlike the doleritic material at Africanders Kloof, the regolith consists of locally sourced sandstone, is very angular, and lacks weathering rinds.

4.2.2. Terrace 2

Terrace 2 typically overlaps or is inset within T1 on both banks in the Wilgerbosch River and Africanders Kloof (Figs. 6, 8, 13, 14), representing the second thickest terrace deposits after T1. Terrace 2 is present overlying bedrock in the first-order Wilgerbosch Kloof and again in the lower valley (see CS-2-7, 9 and 12: Fig. 10). Three main facies associations were defined: (i) 3.3 m of palaeochannel deposits carved into T1 that comprises pedogenically altered, matrix-supported gravels and sands with varied bedding characteristics (Fig. 8: AK-7). (ii) Thick beds (up to 0.95 m) of pedogenically altered, matrix-supported or clast-supported doleritic gravels and cobbles. These deposits overlie bedrock because T1 has been completely stripped in some locations (see AK-8 and 15: Fig. 8). Matrices are primarily composed of ferruginous sands and exhibit strong magnetic susceptibility (AK-8 unit B: $X_{LF} = 91$: Table A.4). These deposits are almost exclusively located in portions of the Africanders Kloof valley proximal to eroding dolerite tors (Fig. 2). Inset deposits also occur as a wedge inset within T1, at the base of knickzone 2 representing the maximum traceable upstream limit of T2 at Africanders Kloof (Fig. 5A). (iii) Deposits of matrix- or clast-supported gravels, cobbles, or boulders interspersed by sand units of varying thickness (0.1–1.5 m) and bedding, and finally, silty sands.

Terrace 2 is overprinted by calcrete up to 10 cm thick (AK-12: Fig. 8). In summary, the principal micromorphological characteristics of the carbonate cements include: (i) minimal fabric expansion indicating

Table 2
Results of OSL analyses for terrace sediments from Africanders Kloof.

Sample	Log/unit	Terrace	Water content (%)[a]	K%	U (mg/g)	Th (mg/g)	Cosmic Ray dose rate (Gy/ka)	Total dose rate (Gy/ka)	n[b]	σ_{OD} (%)[c]	D_e (Gy)[d]	Final age (ka) (1 σ)
LV-509	AK-4/D	AKH-B	2.5	2.51 ± 0.06	2.64 ± 0.07	14.53 ± 0.26	0.21 ± 0.01	4.22 ± 0.66	46	34	34.7 ± 1.9	8.2 ± 1.5
LV-515	AK-11/E2	2	2.3 *15 ± 5	2.1 ± 0.05	2.55 ± 0.06	11.83 ± 0.21	0.17 ± 0.01	3.18 ± 0.34	61	27	54 ± 5.4	17 ± 2.5

[a] Measured field water content. *LV-515: mean water content of 15 ± 5% was assigned because of evidence for a period of prolonged saturation by groundwater.
[b] Number of aliquots used in final age calculation.
[c] Overdispersion parameter.
[d] D_e values calculated using Central Age Model following protocol of Arnold et al. (2007).

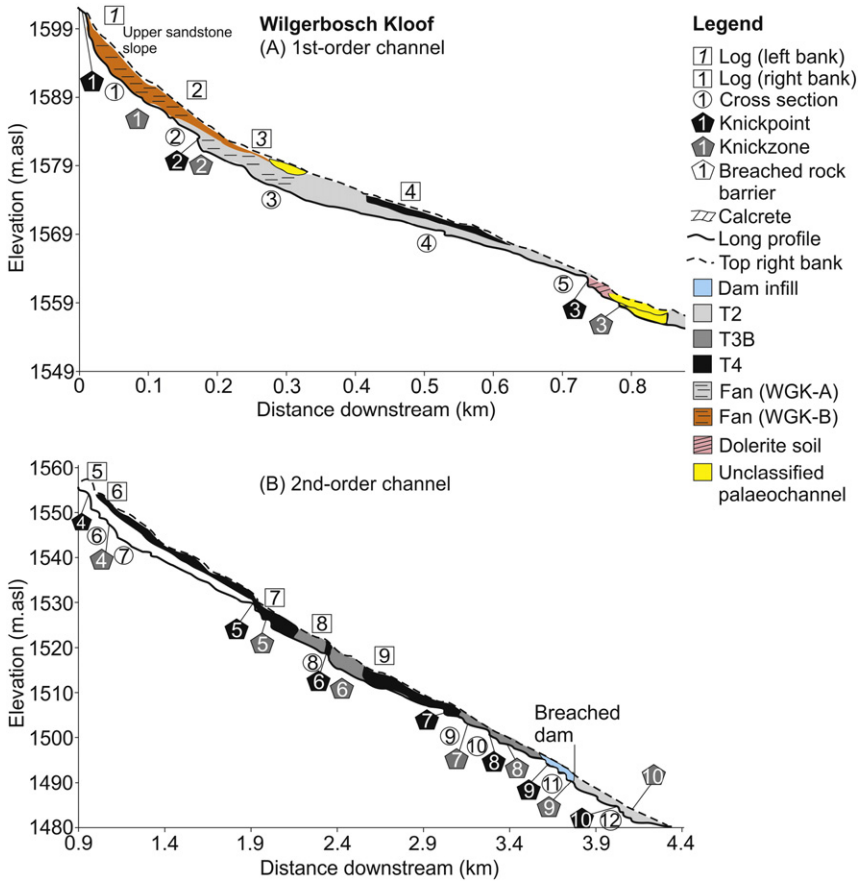

Fig. 9. Wilgerbosch Kloof long profile divided up according to: (A) first-, and (B) second-order channels. Displayed are (1) longitudinal limits of valley fills in relation to channel knickpoints (black hexagon), knickzones (grey hexagon), and breached rock barriers (white hexagons); (2) locations of valley cross sections (Fig. 10); and (3) locations of sediment logs (Fig. 11).

host sediment grains are cemented together rather than pushed apart by calcite growth; (ii) coated lithic grains and grains of secondary carbonate; (iii) root traces; (iv) no evidence for grain etching or quartz replacement by calcite; (v) inset laminated clay coatings; and vi) localised zones of decalcification (Oldknow, 2016). The calcrete occurs at greater height in the terrace profile at Africanders Kloof (up to 6 m, though usually 2.3–2.5 m: Fig. 8) than in the Wilgerbosch River (1.4–1.6 m: Fig. 13). Above the calcrete (230–260 cm: AK-12; Fig. 8), a light brown palaeosol (7.5YR 6/3) with a weak subangular blocky structure is present. The A horizon has been stripped by erosion reflected in the unconformity at 2.65 m (Fig. 8: AK-12). Its micromorphological features include channel-like pores that are lined by calcite hypocoatings as well as inset laminated clays (Oldknow, 2016). Terrace 2 in the upper Wilgerbosch Kloof lacks calcrete, but a similar palaeosol including a light brown (7.5YR 6/3) Bt horizon is preserved but with an overlying light grey (10YR 6/2) A horizon intact (Fig. 11: WGK-2-6).

4.2.3. Terrace 3A

Terrace 3A overlaps and is inset within T2 reaching a maximum thickness (3 m) in the gorge (see GG-1, Fig. 13), but is absent from the upper 1.5 km of Africanders Kloof (Fig. 5A) and Wilgerbosch Kloof altogether (Figs. 9-11). The facies primarily consist of pedogenically altered gravels, sands, and silts. Terrace 3A is less cemented than T2, but exhibits a comparable range of X_{LF} values (34–95), the highest of which occur in areas proximal to dolerite (AK-12, 15: Fig. 2 and Table A.5).

4.2.4. Terrace 3B

Terrace 3B is inset within T2 in the lower Wilgerbosch Kloof (Fig. 10: CS-8 and 10; Fig. 11: WGK-7-8) and contains deposits of sand and matrix-supported gravel. The X_{LF} values range from 36 to 49. WGK-7 exhibits consistently higher D_{90} values (1389–1622 μm) compared with WGK-8 (666–843 μm: Table A.5). Unlike T3A, incipient soil development with no cementation is present (Oldknow, 2016).

4.2.5. Terrace 4

Terrace 4 is inset within T1, T2, T3A, and T3B (Figs. 6, 10, 14), extending into the headwaters of both tributaries, though at Africanders Kloof T4 is absent upstream of the first breached rock barrier (Fig. 5A). Unit AKH-D, the only unit to overtop this barrier, buries a palaeochannel associated with T4 (0.75 km downstream). Downstream of knickpoint 2, T4 occurs as discontinuous pockets burying the earlier terraces. In the second-order channel, T4 overlaps T2 and, with the exceptions of CS-10-12 (Fig. 6), is situated above the calcrete; whereas in the third-order channel, T4 rests on bedrock (Fig. 5C; AK-16: Fig. 8). At Wilgerbosch Kloof, T4 rests on bedrock in the lower second-order channel (Fig. 9B; CS-8-9: Fig. 10).

Terrace 4 consists of four distinct facies groups with distinctive magnetic properties (Table A.6): (1) Gleyed, thick units (up to 1.7 m) of fine-grained sediments that lack any fossilised plants or shells. X_{LF} values are typically much lower than T1-T3 (12–51) and grain D_{50}, with two exceptions (AK-10 unit C and WGK-5 unit E) is <65 μm. (2) Unaltered, thickly laminated sands or silts (D_{50} = 185–1061 μm) that exhibit strong magnetism compared with group 1 (X_{LF} = 38–63). (3) Discontinuity-bounded units (up 1 m thick, but commonly <0.75 m) of silty clay (D_{90} = 27–39 μm), silty sand (D_{90} = 173–266 μm), or sandy silt (D_{50} = 65–216 μm) containing plant macrofossils and/or bivalve shells. The X_{LF} is predominantly very low (11 − 32) with the exception of AK-16 (45–75). (4) Clastic, nongleyed units of matrix (matrix D_{50} = 9–955 μm) or clast-supported gravels that often display inverse grading and weak magnetism (X_{LF} = 13–27). At some locations, an abandoned channel is evident (Fig. 6: CS-6-8; Fig. 10: CS-8).

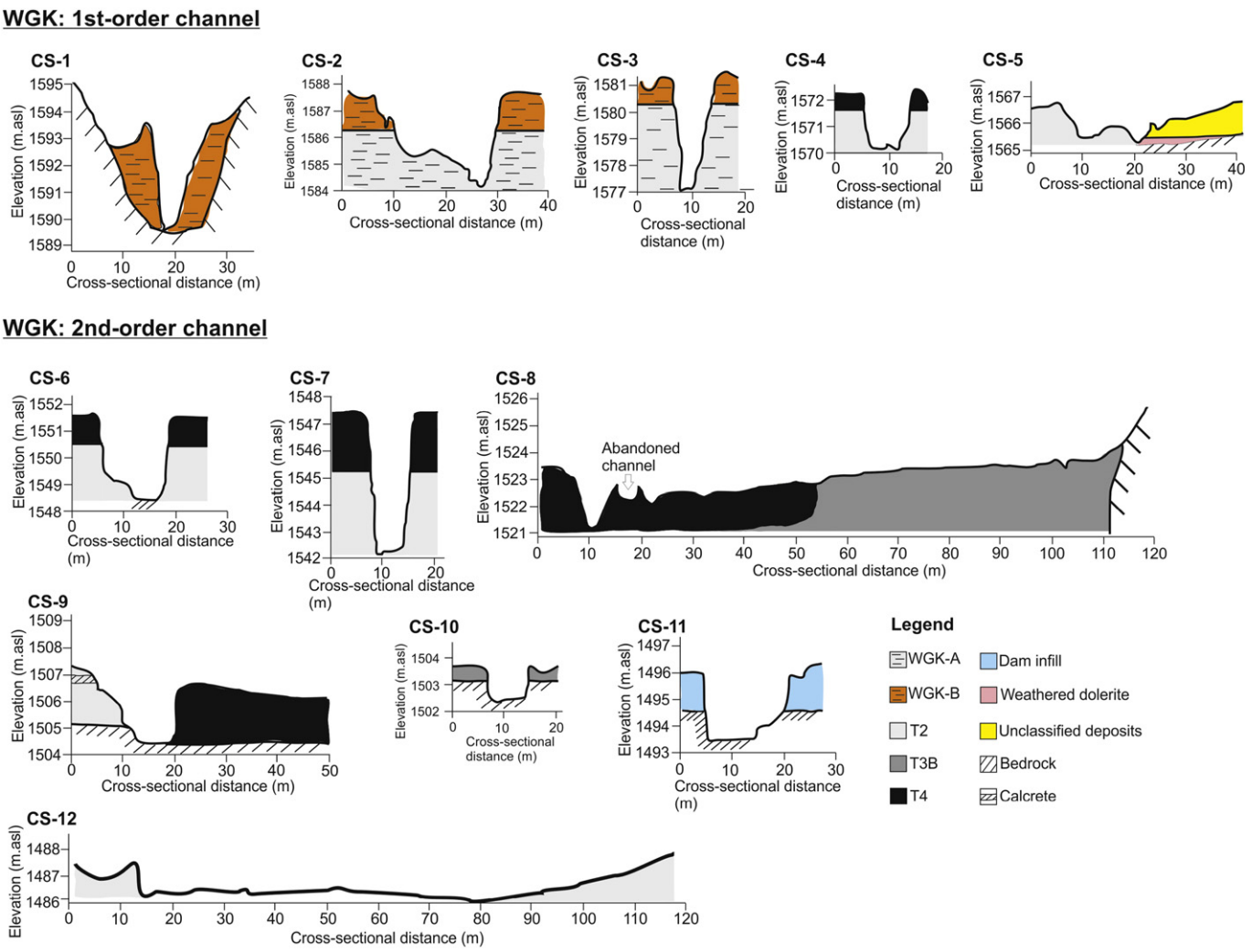

Fig. 10. Valley cross sections showing stratigraphic relations of terrace fills at Wilgerbosch Kloof.

The first and second facies groups are exclusively located in the low-order channels of Africanders and Wilgerbosch Kloof (AK-8, 10 and 13: Fig. 8; WGK-5-6: Fig. 11). The third and fourth facies groups are pervasive in the higher-order channels. For example, in the Africanders third-order channel, the fine-grained units are typically less thick than group 1 deposits (AK-16, Fig. 8), contain plant macrofossils, but are also separated by thin gravel units (0.05–0.15 m thick), and finally, display sharper bed contacts with fine-grained, organic-rich horizons. Up to three such organic-rich units occur in the higher-order channels (WGR-2), but two are represented more widely occurring at a maximum depth of 2.3 m below the terrace surface (WGR-1 units C and E; WGR-2 units H1 and H3; WGR-3 units G and L: Fig. 13). These organic-rich units are interspersed by the thicker, gravel units (group 4).

4.3. Dating results

The representative results of single aliquot equivalent dose (D_e) measurements for both OSL samples are shown in Fig. 15. The rapid initial decay of the OSL signal is indicative of a signal dominated by the fast component (Fig. 15A and B). Sample LV-509 exhibits recuperation ($y > 0$), but this is within 5% of unity. The dose response curves show that D_e values were obtained from the linear part of the growth curve (Fig. 15C and D). Table 2 summarises key results relating to sediment chemistry, water content, degree of overdispersion, and final burial age (ka). The sample from headwater unit AKH-B (LV-509) indicates a final burial age of 8.2 ± 1.5 ka. In contrast, the sample from T2 (LV-515), 1.2 km downstream, is much older indicating that final burial took place around 17 ± 2.5 ka. An AMS ^{14}C date of 0.44 ± 0.04 ka (P-37289) was obtained from fossilised *Juncus* stems at WGR-1 (unit E: Fig. 13).

5. Discussion

5.1. Chronological data

An obvious limitation of this study has been the very low success rate for the OSL and radiocarbon samples. The lack of repeat dates from stratigraphically coeval and bracketing horizons prevents external evaluation of samples LV-509, LV-515, and P-37289.

Samples LV-509 and 515 passed standard screening protocols and additional checks such as the thermal quenching of quartz to assess quartz purity (Shen et al., 2007; Oldknow, 2016). In spite of the large grain-size windows used, overdispersion values are surprisingly modest (Figs. 15E and F) compared to those reported in other fluvial settings (Rodnight et al., 2006; Lyons et al., 2013). Sample LV-509 serves as a preliminary indicator of the age magnitude of the headwater deposits at Africanders Kloof, whilst LV-515 provides a preliminary maximum age on the termination of T2 aggradation. An estimated moisture value of 15 ± 5% was used for LV-515 because of suspected influences from groundwater at outcrop AK-11 (S. Tooth, University of Aberystwyth, pers. comm; Oldknow, 2016).

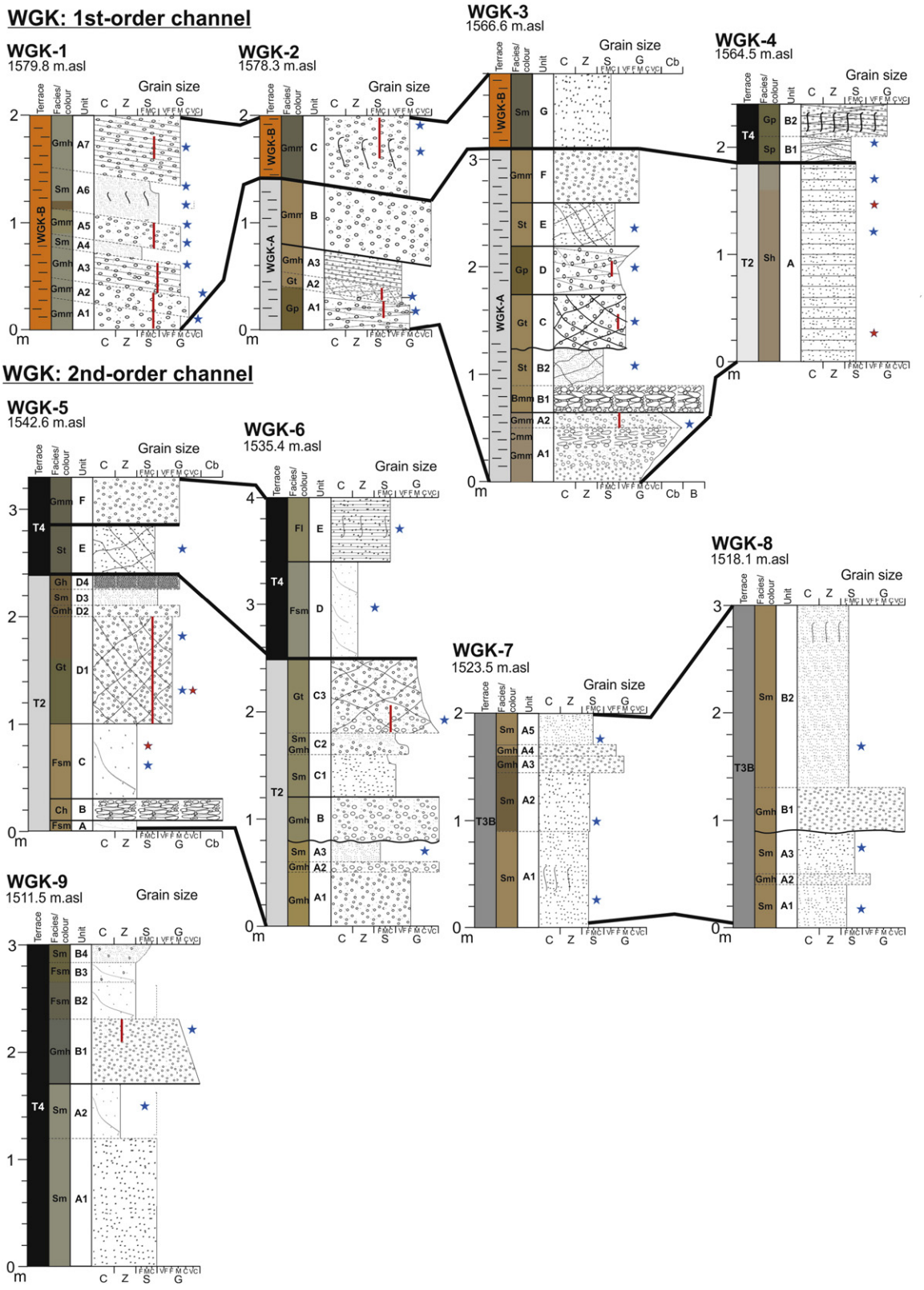

Fig. 11. The alluvial succession at Wilgerbosch Kloof.

The AMS date (P-37289) has two sources of uncertainty associated with it: (i) local groundwater chemistry is likely to have been enriched in calcium supplied by the dolerite (Botha and Fedoroff, 1995), which was taken up by the *Juncus* plants. Consequently, this age may possess a hard water error, meaning that the true age is younger than 0.44 ± 0.04 ka (Peglar et al., 1989). (ii) Plant material may have been inherited from upstream. However, given the depositional environment of this unit (WGR-1 unit E: Table 2), the dated plant material most likely died in situ. Therefore, P-37289 provides a preliminary indication of (i) the minimum age constraining the accretion of unit E and (2) a

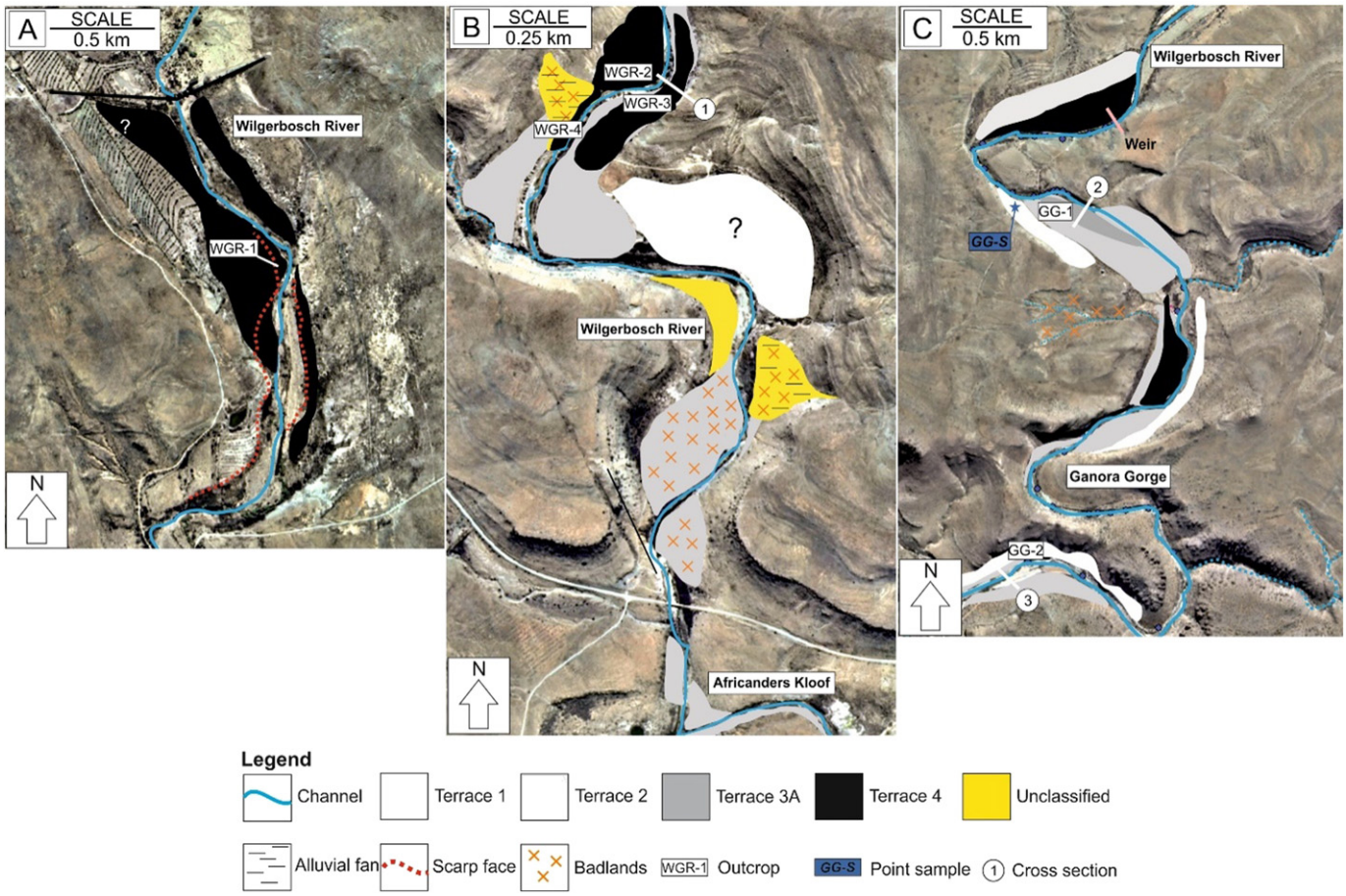

Fig. 12. Annotated digitised aerial photographs of three reaches of the Wilgerbosch River following the order presented in Fig. 2. The physical extent of each major terrace, outcrop, and cross section locations are shown.

maximum age constraining incision of T4. Withstanding the caveats outlined, these three dates are used to propose some tentative hypotheses about the sequence of terrace development.

5.2. Discontinuous valley fills

5.2.1. Africanders Kloof

The interpreted depositional environments for the different facies associations are detailed in Table A.1 (Appendix A) and outlined in the following text. The valley surface that slopes away from the contemporary gully banks (CS-1 and 2: Fig. 6) is a clear indication of alluvial sedimentation around the gully rather than slope-dominated deposition.

The coarse gravel facies associated with unit AKH-A probably reflect two modes of deposition in the upper and lower flow regimes respectively: (i) sheet-flood deposits in a terminal gully system and (ii) the latter stages of flow where it separates into small channels that incise the underlying sediment sheet (Bull, 1972). Unit AKH-A occurs immediately downstream of a major hillslope gully (incised into bedrock), and thus the abrupt change in slope gradient and loss of confinement are conducive to terminal channel processes and fans.

The sediments of AKH-B reflect a range of depositional conditions. The association of bedded and lenticular gravels at section AK-1 (Fig. 7) likely reflects sheet-flood deposits and their subsequent incision as noted for unit AKH-A. Downstream, thicker units of matrix-supported gravel (>0.3 m) reflect high energy conditions of emplacement, probably low plasticity debris flows (Sharp and Nobles, 1953; Varnes, 1978). The lack of discernible trends in particle size with depth at AK-2-4 may reflect a laterally mobile floodout distributary channel. In this case, the trough cross-bedded sands (AK-3 unit A2) probably reflect channel bedforms such as three-dimensional dunes (Miall, 1996). Grenfell et al. (2012) proposed that migration of distributary channels could be tracked by the location of coarser deposits. In this case, the position of outcrops (AK-2-4) is likely capturing lateral differences in sedimentology associated with a distributary system. The occurrence of bedded rather than massive sands and gravels at AK-4 may reflect slower aggradation rates toward the floodout margin. On the basis of OSL age LV-509, aggradation of AKH-B terminated after 8.2 ± 1.5 ka. This age serves as a preliminary maximum age on incision of the dolerite intrusion (breached rock barrier 1).

The first occurrence of unit AKH-C upstream of the break in terrace slope (Fig. 5A) implies that the impetus for incision of AKH-B may have been exceedance of a slope threshold (Schumm, 1979). The inversely graded package of sands, then matrix-supported, very coarse gravels (AK-2: Fig. 7) represent a renewed phase of floodout progradation, confirmed in the progressive reduction in gravel content downstream (AK-2-4). The clayey silt deposits with no coarse material at AK-4 reflect much lower rates of aggradation at the distal margin of the floodout (Nichols and Fisher, 2007). On the basis of minimal if any fossilised plant material, the black colouration of unit AKH-C, and the presence of charcoal fragments, Oldknow (2016) proposed that wildfire may have stripped the vegetation cover on floodout unit AKH-C, priming its surface to incision reflected in the palaeochannels associated with AKH-D. Because sedimentation had reached the top of breached rock barrier 1 during emplacement of AKH-C, sedimentation associated with unit D was able to overtop it. The magnetic susceptibility of the floodout units are typically much higher than published values for dolerite (Rowntree and Foster, 2012), which Oldknow (2016) attributed to lithogenic and pedogenic magnetite.

In summary, the geomorphology and sedimentology of the headwater valley fills exhibit some significant similarities to the floodouts

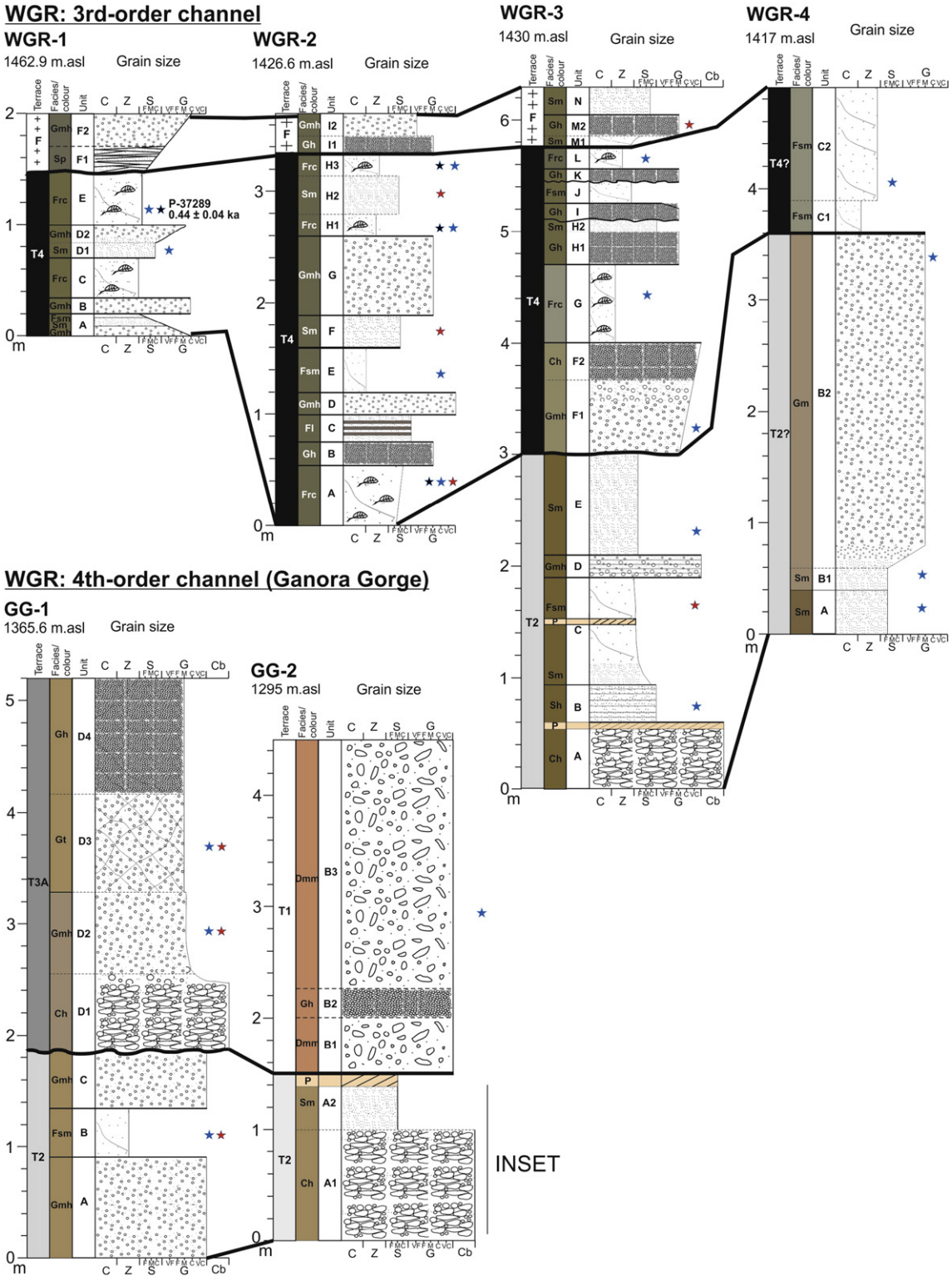

Fig. 13. The alluvial succession in the Wilgerbosch River and Ganora Gorge.

analysed by Grenfell et al. (2014). Floodout behaviour in the Africanders Kloof headwaters has largely been controlled by a lithological impediment crossing the valley. As a result, gullies have been prone to backfilling upstream behind this barrier, but channel avulsions have been less significant than those in the Jackal and Gordonville valleys (Grenfell et al., 2012). It follows that the Africanders Kloof headwaters, prior to the breaching of this rock barrier, were largely unresponsive to phases of regional terrace incision recorded in the higher order channels (Section 5.3).

5.2.2. Wilgerbosch Kloof

The headwaters of Wilgerbosch Kloof preserve two distinct phases of fan emplacement that are morphologically similar to the floodout at Africanders Kloof (see CS-1-3: Fig. 10). The coarsest facies of WGK-A

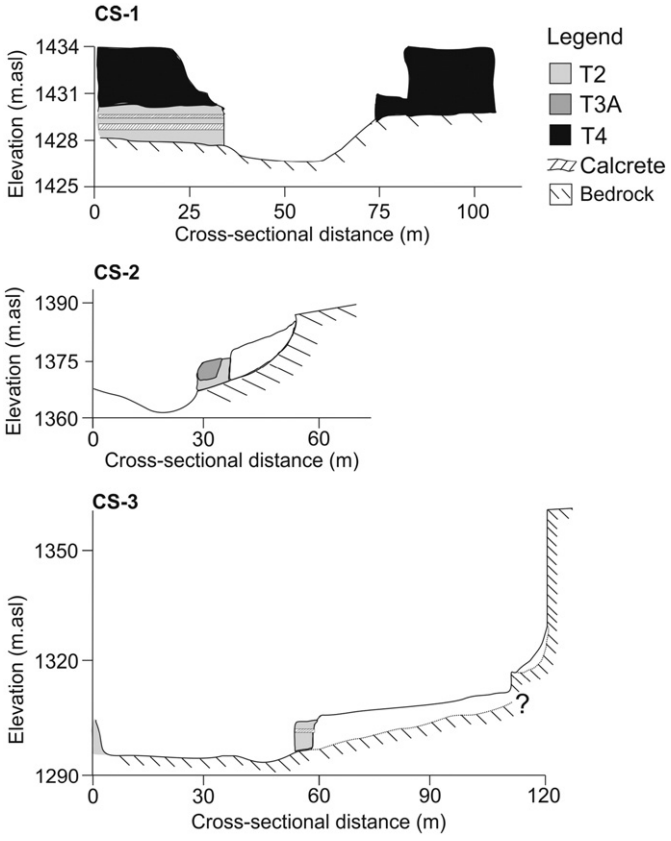

Fig. 14. Valley cross sections at locations shown in Fig. 12 showing stratigraphic relations of terrace fills in the Wilgerbosch River (CS-1) and Ganora Gorge (CS-2 and 3).

are interpreted as debris flows that cascaded off the steep sandstone slope upstream (Fig. 9A). Inverse grading structures in this context likely reflect progradational features; but compared to the floodout at Africanders Kloof, channel deposits are more common here. Sharp bedding contacts between distinct lithofacies accompanied by subtle changes in soil colour (WGK-3: Fig. 11) indicates episodic fan aggradation with periods of minor intervening pedogenesis (Oldknow, 2016).

The deposits of WGK-B reflect emplacement by debris flows and lower energy slopewash processes. The downstream decline in unit thickness and grain size reflects fan progradation (Figs. 10 and 11). The magnetic susceptibility values for this unit correspond to published values for sandstone (Rowntree and Foster, 2012).

Unlike at Africanders Kloof, the fan sediments here were shown to be a source of downstream valley fill because of the absence of any geological barriers (Oldknow, 2016). Thus, the palaeofan has been shown to be linked to base level changes downstream. In addition to the field description of the palaeosol overprinting T2 (Section 4.2.2), Oldknow (2016) identified high concentrations of fine-grained magnetite in the palaeosol overprinting the fan sediments (WGK-A) and T2 (stage 4: Section 5.3), thus indicating a concordant phase of soil development.

5.2.3. Wilgerbosch River

The facies at WGR-4 indicate deposition in an alluvial fan. Unlike the headwater fans (Sections 5.2.1–5.2.2), the strong slope-channel coupling in the Wilgerbosch River (Fig. 12) means that fan aggradation is likely to have occurred in response to changing channel base level.

5.3. Terrace fills of the Wilgerbosch River and its tributaries

To demonstrate the sequences of terrace aggradation, soil development, and incision, the three valley settings are depicted for each phase. The following 11-stage model (Figs. 16 and 17) is proposed, based on the analysis in Section 4.2.

Stage 1: The fine-grained nature of T1 sediments exposed in the first-order gully at Africanders Kloof implies low energy sedimentation. The fact that the valley slopes toward the contemporary gully rather than away from it implies a colluvial rather than alluvial origin. In this case, the inverse grading characteristics may reflect size selective transport, with fines being preferentially winnowed from colluvium stored on slopes, followed by emplacement of coarser material either caused by (i) supply exhaustion of fine sediment or (ii) an increase in magnitude of overland flow. The magnetic susceptibility values for this sediment package more closely correspond to published values for sandstone (Rowntree and Foster, 2012), also implying a local slopewash origin. The occurrence of small infilled palaeogully structures implies that the slopewash sediment was episodically cut and filled. The lower magnetic susceptibility values compared to the floodout deposits just 100 m upstream, in concert with the sedimentological and morphological evidence, clearly demonstrate that the floodout was not a significant source of downstream valley fill. In the second-order channel, the basal horizontally bedded gravels may evidence ephemeral fluvial activity reworking some of the slope material from upstream. The diamictic sediments that comprise T1 in the gorge (GG-S, GG-2: Figs. 12C and 13) also reflect slope-dominated sedimentation, but the coarser nature of the facies here relative to Africanders Kloof is probably a feature of the higher slope-channel coupling. The dominance of sandstone clasts over dolerite implies locally sourced regolith rather than fluvially transported material from upstream. The angular nature of this regolith and absence of weathering rinds attests to the dominance of physical rather than chemical weathering – probably frost-shattering along bedding planes and joints. The vertical orientation of clasts that 'float' within a poorly sorted matrix indicates mass-wasting processes. The evidence for physical weathering and the diamictic nature of the sediments may reflect periglacial, activity such as gelifluction, with seasonal freezing and thawing of surficial layers of the groundmass (Benedict, 1976). The clast-supported gravel unit (GG-2, unit B2: Fig. 13) within this context, likely reflects the washing out of fine material by melt processes. In summary, this stage is characterised by colluviation and mass wasting with suppressed fluvial activity relative to stage 2.

Stage 2: The first incision phase (T1) was characterised by formation of a deep and extensive channel network on the basis of (i) the upstream extent of T2 at the confluence between the first- and second-order channels at Africanders Kloof; (ii) the fact that T1 has either been completely stripped, or only 0.8 m remain, overlapped by T2; and (iii) the depth of infilled palaeochannels sourced from the slopes that conform to the elevation of channel deposits (T2) on the valley floor. The occurrence of T2 at Wilgerbosch Kloof indicates connectivity was established with the upper parts of the system.

Stage 3: Up to 6 m of alluvium accumulated during the aggradation of T2. In particular, the association between the limited preservation of T1 and very coarse facies (groups 1–2: Table A.1) implies high energy flow conditions, probably debris flows. The proximity of these deposits to dolerite tors is significant as the tors constitute resistant landscape elements and produce steep topography conducive to generating rapid runoff (Fig. 2). During this phase, the evidence indicates a phase of connectivity between the slopes and valley floors. The facies associated with group 3 reflect channel and overbank sediments and thus are genetically and architecturally different from the sediments that comprise T1. The OSL age LV-515 indicates that aggradation of T2 at AK-11 (Fig. 8) terminated in the deglacial period (17 ± 2.5 ka). If this age is accurate, then T1 was deposited prior to this date, possibly at or around the time of the LGM. In summary, stage 3 is characterised by an initial phase of slope-channel connectivity caused by expansion of the channel network. Aggradation of the valley floors then appears to have occurred in response to the fluvial network becoming choked with sediment.

Stage 4: Following the aggradation of T2, a 6-cm-thick calcrete horizon formed. The micromorphological features (Section 4.2.2) are consistent with the 'beta fabric' (biologically dominated) calcrete variety (Wright et al., 1988; Renaut, 1993; Oldknow, 2016). The formation of

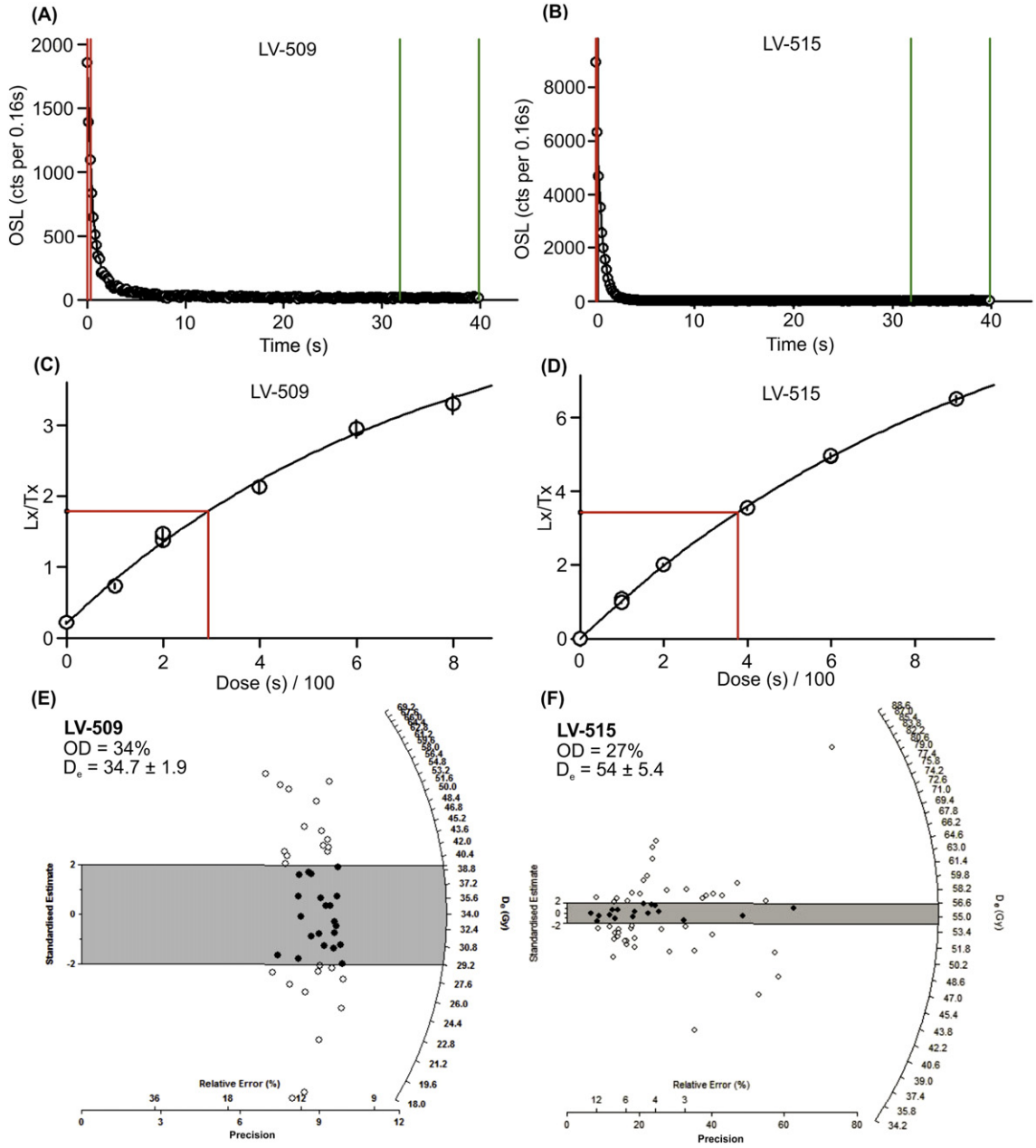

Fig. 15. Plots showing representative OSL results for samples LV-509 and 515, including: (A) and (B) the natural OSL signal against stimulation time showing that the OSL signal is dominated by the fast component; (C) and (D) dose response curves that show D_e values derived from the linear part of the growth curve. L_x/T_x is the OSL signal from the aliquot (L_x) normalised by the signal from a fixed test dose (T_x); and (E) and (F) radial plots showing typical D_e distributions for each sample. The grey bar denotes the dose value used for age calculation, using the Central Age Model (CAM) following the decision-making protocol of Arnold et al. (2007).

such calcrete types occurs in association with phreatic root systems that are accessing a deep or near-surface water table. Where the root networks come into contact with the water table, they spread laterally and subsequent calcification, dominated by biological fixing, generates a thin but laterally extensive calcrete horizon (Wright et al., 1995). Zones of decalcification accompanied by illuviated inset laminated clay coatings in the calcrete and palaeosol above attest to a shift in soil conditions (Yaalon, 1997). This is because clay illuviation is incompatible with carbonate-fixing conditions, as dissolved Ca^{+2} within soil water causes clay particles to flocculate (Kemp, 1985; Rose et al., 2000). This indicates that following calcrete development, water in the vadose zone drained freely through the profile as a result of a reduced water-table level. The presence of a second, thinner rhizogenic calcrete horizon elsewhere (see WGR-3 unit A: Fig. 13) indicates fluctuating groundwater levels. Because this variety of calcrete may be taken as a surrogate for the maximum upper limit of the water table, this indicates that the water table rose up to 6 m above bedrock in the tributaries (Africanders Kloof and the lower Wilgerbosch Kloof), whilst a maximum of 1.5 m above bedrock in the Wilgerbosch River was attained. The extensiveness of this calcrete attests to vegetated floodplains and slopes during stage 4 (Oldknow, 2016). The calcrete acted to blanket (Fryirs et al., 2007) the sediments associated with T1 and T2, with the exception of the upper Wilgerbosch Kloof where no calcrete is present.

Pedogenic calcrete has been reported elsewhere in the Sneeuberg where it cements deeply weathered gravels (Holmes et al., 2003) that are substantially older (48.9 ± 5.4 ka; Boardman et al., 2005) than the Wilgerbosch valley fills (17 ± 2.5 ka). The lack of well-dated modern

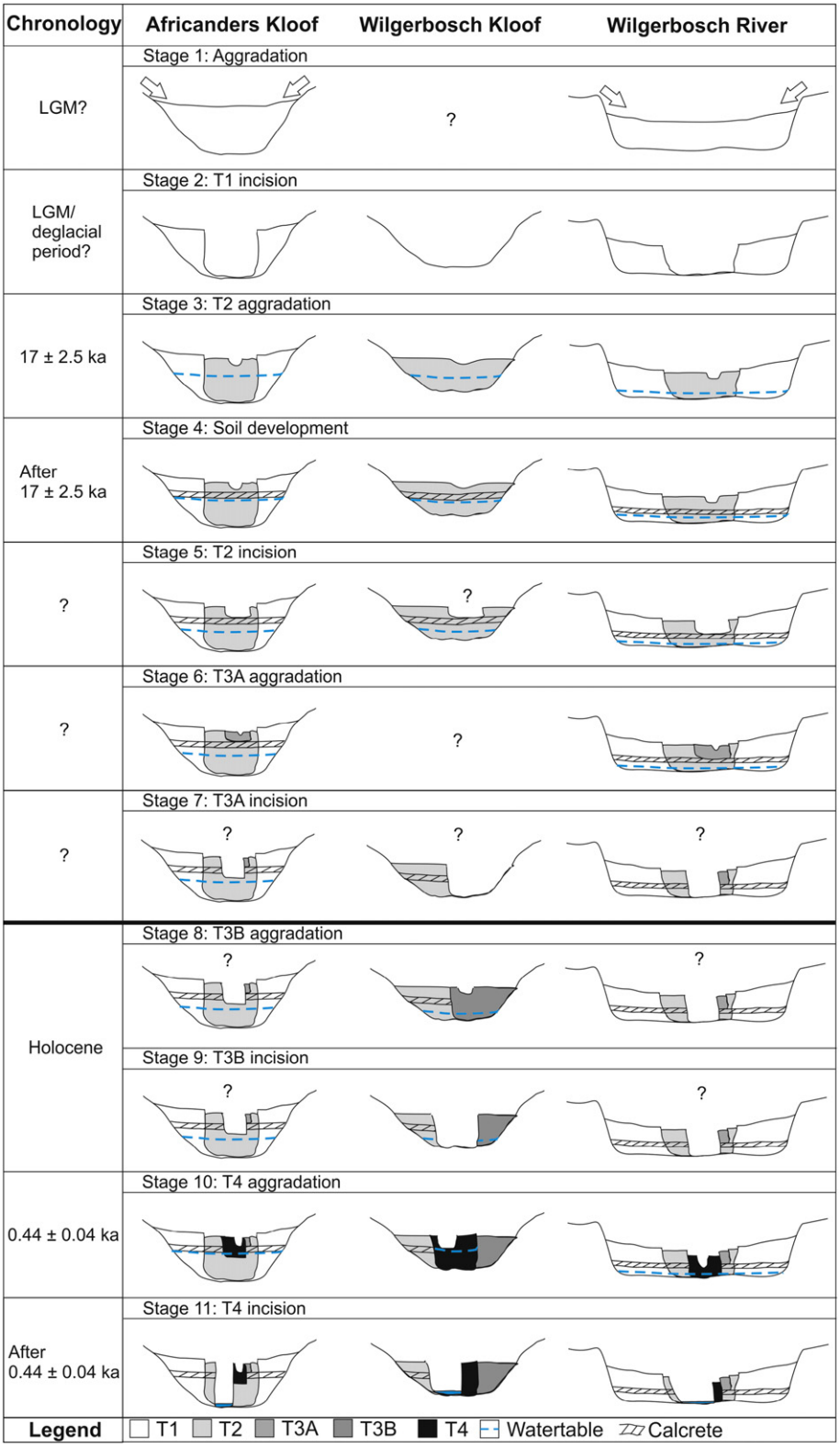

Fig. 16. Illustrated stages of terrace development in each of the three tributaries investigated.

analogues of rhizogenic calcrete formation make it difficult to estimate rates of formation of such profiles (Wright, 1990), but Klappa (1980) reported living roots with calcareous sheaths implying that their formation is likely to be rapid compared to 'alpha fabric' pedogenic calcretes (Candy and Black, 2009). The calcrete in the Wilgerbosch catchment thus appears to have a different genetic origin and age to that reported by Holmes et al. (2003).

Stages 5–7: The presence of an inset third terrace (T3A) is a clear indication that the channels once again incised (stage 5); but because of the cemented nature of the valley fills (T1/T2), incision was limited

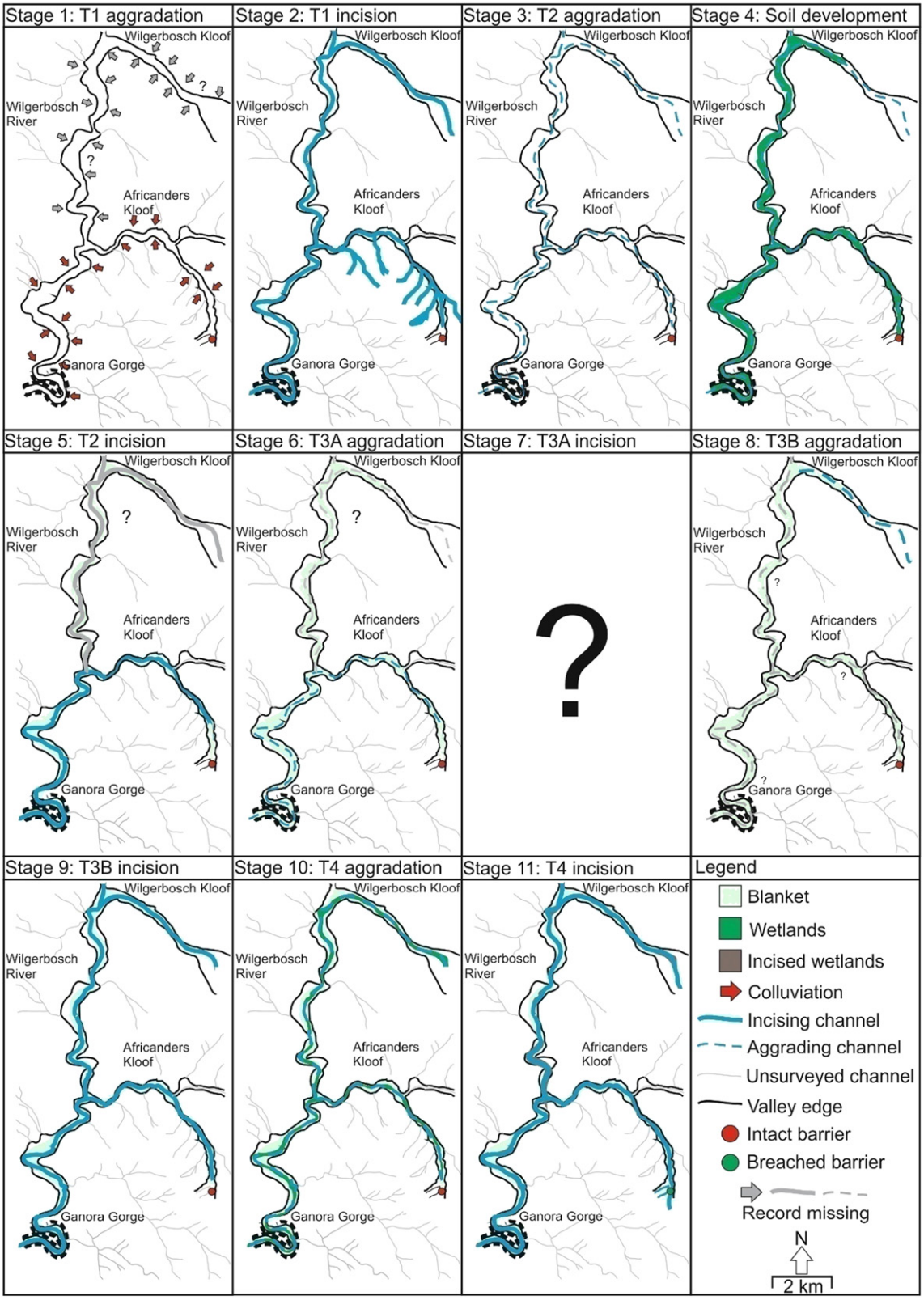

Fig. 17. Palaeoconnectivity for each stage of terrace development derived from analysis of terrace continuity. Grey rather than coloured arrows and solid and dashed lines indicate where gaps exist in the stratigraphic record.

compared to stage 2. The upstream limits of this phase of channel incision are difficult to constrain confidently. The absence of T3A from the upper 1.5 km of Africanders Kloof, the Wilgerbosch River (upstream of the confluence with Africanders Kloof), and Wilgerbosch Kloof could be a matter of preservation or that incision did not extend all the way upstream. The facies deposited in stage 6 that comprise T3A have been interpreted as migrating single-thread channel deposits. The conditions under which T3A incised and the upstream extent of this

incision (stage 7) are unknown because an unconformity separates it from T4.

Stages 8–9: The facies associated with T3B at Wilgerbosch Kloof are interpreted as slopewash and channel deposits (WGK-7 and 8 respectively: Fig. 11). This implies that slope colluvium was washed into the valley floor and redistributed by fluvial activity. Magnetic susceptibility values are lower than those quoted for sandstone, probably reflecting dilution by sediment eroded from mudstone bedrock. The finer grain size of the channel sediments (WGK-8) indicates deposition in a sand-bed stream. Oldknow (2016) distinguished T3B from T3A on the basis of there being only incipient soil development and no cementation. Terrace 3B is therefore probably Holocene rather than Pleistocene in age. Unit T3B was then incised to bedrock level (stage 9). The restricted longitudinal extent of this terrace may either be as a result of low alluvial preservation potential or that this terrace was only deposited in Wilgerbosch Kloof.

Stage 10: T4 contains four distinct facies that indicate large shifts in river activity up until the late Holocene, but the expression of these shifts varies between the different valleys (Table A.1). The gleyed fine sediments (group 1) located in Africanders and Wilgerbosch Kloofs are similar to the mid-late Holocene vlei soils reported elsewhere in the Sneeuberg (Holmes et al., 2003) though these apparently represent pools that formed upstream of floodouts during periods of low flow along the Klein Seekoi River (Grenfell et al., 2014), rather than a continuous low-energy channel system. They represent deposition from suspension in a wetland environment (group 1) but, in contrast with group 3 facies, do not possess organic remains (Table A.1). Oldknow (2016) demonstrated that these units exhibit 'paramagnetism' attesting to dominance of iron sulphides that can form as a result of the dissolution of organic matter (Williams, 1992). On the basis of this evidence and the elevation of the calcrete formed during stage 4, Africanders Kloof has been prone to a higher water table caused by two factors: (i) relatively narrow valleys compared to the Wilgerbosch River and (ii) groundwater discharge from doleritic aquifers (I. Meiklejohn, Rhodes University, pers. comm.).

The second facies group, which buries these gleyed sediments, represents up to 0.8 m of unweathered overbank deposits reflected in their coarser grain size and stronger magnetic susceptibility, which are associated with the palaeochannel shown in CS-6-8 (Fig. 6). The third facies group, which consists of fine-grained sediments but contain plant macrofossils, are interpreted as low energy channel deposits in a wetland but have not been subject to gleying by a near-surface water table to the same degree as group 1. These appear to represent phases of relatively slow aggradation and stability on the valley floors. The last of these preserved phases occurred around 0.44 ± 0.04 ka (P-37289: Section 5.1), which appears to be considerably more recent than the vlei soils along the Klein Seekoi River (Sugden, 1989).

The coarse sediments (group 4) that intersperse these wetland units exposed in the Wilgerbosch River banks are interpreted as channel deposits associated with flood events, with the normally graded finer sand and silt units representing receding flow conditions. The inversely graded sands and gravels are attributed to deposition of coarse material on bars at the channel margins during high flow (Hooke, 2004) and are a feature of contemporary flood deposits in the Wilgerbosch River (Oldknow, 2016). The increasing expression of these flood deposits here (WGR-1-3: Fig. 14) relative to Africanders Kloof (Fig. 8) may have been caused by greater discharge as the high-order channels integrate a larger catchment area. Furthermore, at Africanders Kloof, T4 in the second-order channel is mainly situated above T2, and thus, coarse deposits associated with T2 were not reworked (Figs. 6 and 9). Additionally, unlike the stage 2 incision phase, knickpoint retreat associated with the wetland channel (T4) was apparently not as extensive (stage 10: Fig. 17). Thus, lack of connectivity with sources of slope colluvium resulted in a supply-limited system with respect to coarse sediment. Flood events at Africanders Kloof are thus reflected in overbank sedimentation (group 2); whilst on the Wilgerbosch River, they manifest in the emplacement of much thicker, coarser channel deposits (group 4).

Stage 11: On the basis of AMS date P-37289 (Section 5.1), the incision of T4 probably occurred after 0.44 ± 0.04 ka, where up to 5–6 m deep channels were entrenched. In many places, incision proceeded to bedrock; and at Wilgerbosch Kloof, active knickpoint recession has carved a small inner channel through mudstone in places. This incision phase appears to be reconnecting formerly disconnected reaches of the valleys. For example, the top of a knickpoint formed through the floodout deposits at Africanders Kloof corresponds to the top of breached rock barrier 1 (Fig. 5A). This implies that the breaching of this barrier occurred during stage 11 and thus connectivity was established with the headwaters triggering incision of the palaeo-floodout (Section 4.1.1). In contrast, several of the unsurveyed tributaries remain disconnected from the main channels by wedges of intact valley fill such that they have not responded to the stage 11 incision (Fig. 17).

Erosion has stripped the fills from the Wilgerbosch River valley with remnants preserved in just three reaches (Fig. 12). Currently, aggradation is limited to pockets of inset floodplain (up to 1 m above the channel bed) in wider, low energy reaches upstream of bedrock knickpoints. In the tributaries, badlands previously reported and discussed by Rowntree and Foster (2012) are most common in deposits associated with T4 (Oldknow, 2016).

5.4. Processes and drivers of terrace formation

5.4.1. Base-level change

The Great Karoo has been apparently tectonically stable since the mid-Pleistocene (Bridgland and Westaway, 2008). The Wilgerbosch River has been buffered from effects of sea level fluctuations by the Klein Winterhoek Mountains to the south and the Great Escarpment (Hattingh, 1996).

Alluvial and bedrock incision have been linked to the breaching of geological barriers. On the Klip River, Tooth et al. (2002, 2004, 2007) outlined how resistant dolerite sills and dikes act to anchor upstream river longitudinal profiles. Lateral deposition occurs upstream of barriers in unconfined settings and vertical aggradation in confined settings (Tooth et al., 2013). Partial or complete barrier breaching causes floodplain abandonment upstream and channel incision through relatively soft bedrock underlying the dolerite (Tooth et al., 2004).

In the Wilgerbosch River catchment, the continuity of vertically aggraded terrace fills over the major knickpoints and knickzones portrayed in this study was an indication of catchment-wide phases of aggradation and incision. Whilst rates of fluvial incision through dolerite are unknown, several studies have proposed that barriers can serve as local base levels for 10^4–10^5 years (Tooth et al., 2007, 2013; Keen-Zebert et al., 2013), but the mechanisms of breaching are poorly understood. Springer et al. (2005, 2006) proposed that growth and coalescence of potholes can eventually form narrow and deep channels through the rock mass, whilst Tooth et al. (2013) suggested plucking of joint-bounded blocks as a zone of less-resistant rock is encountered.

Downstream of channel knickzones, the thicknesses of (3–6 m) and stratigraphic boundaries between terrace fills at Africanders Kloof imply that phases of bedrock incision have been highly episodic and potentially brief compared to phases of prolonged alluvial cover, particularly in the first- and second-order channels. Prior to stage 11, the last time that incision could have possibly exceeded the vertical depth of accumulated sediment deposited downstream of channel knickzones here was during stage 2. During phases of alluvial cover, on the basis of the thickness (up to 0.6 m) and extent of clay soil formed on dolerite (Fig. 5), subsurface chemical weathering appears to have been an important process by which barriers were weakened. This would have rendered them susceptible to partial or complete penetration during phases of deep channel incision. An example of this is the incision of breached rock barrier 1 formerly decoupling the headwater floodout from the higher order channels at Africanders Kloof (Fig. 5A). In contrast, alluvial cover over sandstone knickpoints and knickzones is relatively thin (1–2 m), and no soils are preserved on bedrock. These factors imply that

mechanical erosion as a means of barrier incision has been more significant than chemical weathering in these locations.

Thus, in summary, the importance of in situ chemical weathering has emerged as another mechanism contributing to dolerite barrier incision (Tooth et al., 2004) and its importance for interreach scale sediment connectivity (Hooke, 2003), as well as sensitivity of response to downstream adjustments in channel long profile. The knickpoints catalogued in the long sections appear to have comparatively sustained more frequent mechanical erosion owing to locally thinner alluvial cover.

5.4.2. Climate

5.4.2.1. Last glacial maximum. Terrace 1 appears to have been deposited prior to 17.5 ± 2.5 ka (LV-515: Table 2), possibly around the time of the LGM (Bottelnek Stadial). In the nearby Drakensberg, periglacial activity in the form of rock glaciers, glacial moraines, protalus ramparts, and aeolian dust accretions have been reported (Osmaston and Harrison, 2005; Lewis, 2008). In particular, head deposits have been found in the eastern Drakensberg above 1800 m asl and may indicate former mean annual average temperatures (MAAT) of <6 °C (Lewis, 2008). No minimum age for these deposits in the Drakensberg has been obtained as yet, but maximum ^{14}C ages of 40, 37.2, and 26.2 ka have been obtained at different locations (Hanvey and Lewis, 1990; Lewis, 1999, 2005) placing the genesis of gelifluctate fills at or close to the MIS3/2 boundary.

The characteristics of these 'head deposits' (Lewis, 2008) closely correspond to the fills reported in the Ganora Gorge (Section 5.3), though the gorge is some 500 m lower (1295 masl) than the Drakensberg. This may indicate that temperatures were comparably low (MAAT = 6 °C or lower) even at this elevation.

Working on the Masotcheni Formation sediments in the KwaZulu-Natal, Temme et al. (2008) proposed that solifluction was an important colluvial process prior to 29 ka, but that sedimentation halted throughout the LGM. This contrasts with other work that has demonstrated that up to 3 m of colluviation occurred during MIS2, though interspersed by four palaeosols implying variable climatic conditions (Clarke et al., 2003). Lyons et al. (2013), working on tributary fan sediments of the Blood River, also suggested that colluviation started prior to 22 ka; whilst Lyons et al. (2014) statistically demonstrated a link between arid, cold conditions (Partridge et al., 1997) after 28 ka and colluvial sedimentation on the Modder River.

Quantitative estimates of palaeo-preciptitation for the Sneeuberg are unavailable, but Lewis (2008) proposed that precipitation may have been up to 70% lower than in the Drakensberg during the LGM. A comparable reduction in the Sneeuberg would mean annual totals of 127 mm·a^{-1} relative to present totals (Grenfell et al., 2014). Subdued fluvial activity is reflected in the facies of T1 relative to T2 and so climatic conditions may have been relatively arid. Aggradation in other drylands like the Mediterranean has often, though not always, taken place during climatically cold, dry phases (Petit et al., 1999; Macklin et al., 2002), even in areas that exhibit different rates of tectonic uplift (Macklin et al., 2012). Various authors have proposed that this has been achieved through the effect of climate on vegetation cover, enhanced mechanical weathering, rock breakdown, and mass wasting increasing sediment supply (Gil García et al., 2002; Woodward et al., 2008; González-Amuchastegui and Serrano, 2013; Soria-Jáuregui et al., 2016). In the SW USA, historical arroyo infilling has been linked to phases of declining rainfall (Love, 1977; Hereford, 1986; Balling and Wells, 1990; Hereford and Webb, 1992). Terrace 1 in the Wilgerbosch catchment appears to have aggraded under cold and dry conditions relative to stages 2 and 3.

5.4.2.2. Deglacial period. The timing of channel entrenchment in stage 2 probably occurred prior to 17 ± 2.5 ka. The impacts of transient changes in climate are widely understood to have the most impact on erosion and sediment transport caused by changing rainfall/vegetation phase relationships (Knox, 1972; Bull, 1991; Tucker and Slingerland, 1997; Inman and Jenkins, 1999; Zhang et al., 2001; Molnar, 2004). The depth of incision associated with stage 2 reflects increasing flood magnitude. This could relate to increasing rainfall around the transition of the LGM/deglacial period but also to changing dynamics of sediment supply (Section 5.4.3). The switch to aggradation in stage 3 is proposed to be primarily a complex response (see Section 5.4.3), but some broad inferences about climate in stage 4 are now proposed in light of general climatic patterns and characteristics from other proxy records for this time period.

Though elevated groundwater levels in stage 4 were partly a feedback response to infilling of the valleys (Section 5.3), evidence for comparably high levels during stage 1 was not found. This implies that climatically wetter conditions prevailed in stage 4. Lyons et al. (2014) demonstrated that dry conditions persisted up until 15.5 ka. Reported high lake levels between 19.3 and 17 ka at Alexandersfontein just 80 km west of the Erfkroon site (Lyons et al., 2013) may reflect reduced evapotranspiration under cool, relatively 'dry' climatic conditions (Butzer et al., 1973; Butzer, 1984). However, Chase et al. (2015a,b) from a Hyrax Midden record in the Cedarberg, western Cape region, proposed that increasing humidity occurred in the early deglacial period (18–14.6 ka). They have argued that increased flow of warm Agulhas Current waters into the SE Atlantic and reduced northward heat transport in the Atlantic meridional overturning circulation (AMOC) favoured increasing advection of the tropical easterlies (from the Indian Ocean) in the western Cape (Reason et al., 2006). This model suggests that the summer-rainfall zone had expanded across the entire southern portion of the subcontinent during this phase. Had this impacted on the Sneeuberg (320 km farther south than the sites of Butzer and Lyons), enhanced summer-rainfall would have reduced drought-stress for vegetation. The thickness and extent of the calcified rootmats (Oldknow, 2016) indicates wetlands and slope vegetation unmatched by subsequent phases and could in theory reflect not only increasing precipitation amount but shifts in rainfall seasonality. As discussed in Section 5.3 (stage 4), the micromorphological evidence for a drop in water-table following the development of the rhizogenic calcrete implies that relatively arid conditions ensued thereafter.

5.4.2.3. Holocene. Holocene valley fills are a feature of other valleys in the Sneeuberg and wider Karoo, commonly consisting of clastic sediments buried by organic-rich fills similar to the T4 fine-grained units reported earlier (Bousman et al., 1988; Holmes et al., 2003). A key difference between the stratigraphy of the vlei deposits in the Wilgerbosch River and those in the Klein Seekoi is that they tend to be less thick and interspersed by coarse flood deposits. In addition the uppermost vlei accumulation in T4 is considerably younger (0.44 ± 0.04 ka) than that preserved in the Klein Seekoi River (2510 ± 50 Yr BP; Holmes et al., 2003). The age of the underlying flood deposits and vlei soils along the Wilgerbosch River has yet to be established. So far, the oldest date (7790 ± 90 Yr BP) for the organic-rich fills in the Karoo was obtained by Sugden (1989) at Blydefontein, but Holmes et al. (2003) obtained dates no older than 5790 ± 80 Yr BP from vlei soils in the Klein Seekoi headwaters. However, at Sani Top, Lesotho, Marker (1995) reported organic deposits of late Pleistocene (14 ka) age, but then a distinct 'mid-Holocene organic phase' similar to that reported in the Great Karoo (Holmes et al., 2003). This cyclical accumulation of organic-rich sediments supported by palynological evidence has been used to infer moister conditions commencing around 4600 Yr BP (Sugden, 1989), possibly linked to increased summer rainfall. Interestingly, Chase et al. (2015a,b) argued from their Katbakkies hyrax midden record that Holocene climate was variable in South Africa, reflecting variations in tropical easterly flow and the position of mid-latitude westerlies. They propose that periods of increased easterly flow occurred at 6.9–5.6, 4.7–3.2, and 2.7–1.6 cal BP, which overlap with the dates compiled by Holmes et al. (2003). However, as noted earlier, the vlei soils have more recently been discussed in the context of palaeo-floodout systems that are controlled by local valley morphodynamics and base level (Grenfell et al., 2014). The apparently diachronous nature of these

soils may therefore reflect phases of floodout evolution rather than discrete climate events of the regularity indicated by other climatic records (Chase et al., 2015a,b).

5.4.3. Geomorphic thresholds and complex response

Terraces can result from the exceedance of geomorphic thresholds and complex response (Schumm, 1973, 1977, 1979; Patton and Schumm, 1981). For example, phases of floodout progradation at Africanders Kloof were shown to be a feedback response to reduced valley slope and loss of confinement upstream of a dolerite dike. Conversely, phases of incision were found to be related to factors of oversteepening, wildfire disrupting local vegetation cover, and knickpoint retreat. As previous observations have demonstrated, fluvial landforms controlled by intrinsic processes tend to be small (Womack and Schumm, 1977; Houben, 2003; Grenfell et al., 2014).

Some of the valley fills in the Wilgerbosch River catchment, however, constitute much larger features (at least 10 km long). Whilst continuous deposits may have a tendency to reflect catchment-wide changes in the sediment-discharge ratio and therefore some external (allogenic) driver(s), distinguishing deposits within terraces that are the products of allogenic from autogenic forcing is not straightforward (Wang et al., 2011). Only strong allogenic impulses may be sufficient to override local variations in channel slope, sinuosity, and barriers that may otherwise introduce autogenic 'noise' and therefore amplify leads and lags in fluvial response to allogenic drivers (Vandenberghe, 2003; Erkens et al., 2009; Lyons et al., 2013). For instance, the evidence for increased flood magnitude in stage 2 (relative to stage 1) may not necessarily indicate large increases in rainfall (Knox, 1993) but equally exhaustion of sediment supply from slopes, such that channels incised into the valley floor and progressed upstream by knickpoint retreat.

The identification, classification, and quantification of the transitions from allogenic responses to where intrinsic feedbacks and complex response take over in regard to fluvial evolution is important for relating specific sedimentary architectures to appropriate genetic drivers. For example, allogenically forced channel incision may occur; but subsequent expansion of the channel network, as demonstrated in stage 2 (Fig. 17), can produce temporary increases in sediment supply causing channel aggradation and a phase of disconnectivity (Horton, 1945; Montgomery and Dietrich, 1992; Tucker and Slingerland, 1997). Nicholas et al. (1995) applied the term 'superslug' to articulate major changes in sediment supply that produced basin-wide impacts. In the USA, aggradation rates of up to 15 $cm \cdot a^{-1}$ have been reported where 'superslugs' have developed (Trimble, 1983). Hence aggradation can occur because of changing dynamics of connectivity. A similar mechanism may have operated in the Wilgerbosch catchment to trigger a switch from incision (stage 2) to aggradation (stage 3) as T1 was progressively reworked and new stores of colluvium on slopes were temporarily connected to the drainage network. In particular, palaeochannels that headcut upslope linking the deeply weathered dolerite tors to the valley floors at Africanders Kloof in stage 2 appear to have contributed to this aggradation in stage 3. The thickness of colluvium required to trigger aggradation of the magnitude observed in stage 3 would have likely required an extended period of chemical weathering on the hillslopes that probably predated the LGM (Holmes et al., 2003; Decker et al., 2013).

Though the possible role of climate in driving changes in groundwater level has been discussed (Section 5.4.2), the high water table and development of calcified rootmats in stage 4 appear to have equally been a complex response to aggradation and disconnectivity in stage 3 because incised gullies channelize the groundwater discharge from seepage zones (I. Meiklejohn, Rhodes University, pers. comm; Boardman, 2014). The thickness and extent of the calcrete horizon appears to have had significant implications for alluvial storage potential in stages 4–10.

Tributary incision may also lag base-level changes downstream depending on the position of the main channel within the valley floor (Brierley and Fryirs, 1999). This is evidenced by several impounded tributaries in the third-order Africanders Kloof that have not incised (stage 11).

5.4.4. Alluvial preservation factors

Extent of alluvial preservation is controlled by a multitude of factors like incision rates, substrate lithology, lateral channel migration rates, tectonism, and valley morphology (Erkens et al., 2009; Fryirs and Brierley, 2010; Macklin et al., 2012; Keen-Zebert et al., 2013). Erosion of valley fills can introduce spatial and temporal bias in the alluvial record (Lewin and Macklin, 2003).

In the Wilgerbosch River catchment, substrate lithology has been important in direct and indirect ways for alluvial storage capacity. Lithological impediments (Section 5.4.2) have been shown to directly control alluvial storage potential within the Africanders Kloof headwaters, which appear to preserve sediments of greater age than those reported in a first order gully ('Compassberg Kraal') of the Klein Seekoi River (Holmes et al., 2003). Conversely valleys carved into mudstone (i.e., Wilgerbosch Kloof) tend to be wider and less steep (Oldknow, 2016). The presence of an intermediate terrace (3B) here may therefore be a feature of greater accommodation space (Keen-Zebert et al., 2013). However, softer bedrock lithologies are known to generate high sediment yields that can overwhelm stream power and trigger aggradation and backfilling (Bull, 1991; McFadden and McAuliffe, 1997). Therefore, T3B may have been restricted to Wilgerbosch Kloof.

Indirectly, the dolerite bedrock has impacted alluvial preservation capacity by having supplied calcium (Botha and Fedoroff, 1995) from weathering of anorthite that formed calcrete in stage 4 (Oldknow, 2016). This calcrete has acted to 'blanket' (Fryirs et al., 2007) and thereby 'disconnect' T1 and T2 sediments, the latter exhibiting the most extensive preservation. This may account for why there is such good preservation of the oldest part of the terrace record in the gorge, which ordinarily may be expected to preserve younger alluvial/colluvial units (Harden et al., 2010; Harvey et al., 2011). Conversely, the lack of calcrete in the upper Wilgerbosch Kloof is probably to do with the dominance of sandstone and mudstone rather than dolerite and thus the earliest terrace has been eroded. Additionally, sediment derived from mudstone has been shown to be particularly erodible (Rienks et al., 2000).

The thickness of the calcrete, particularly at Africanders Kloof, appears to have had a significant limiting effect on depth of channel incision after stage 4, thereby enhancing disconnectivity. This meant that accommodation space in subsequent phases of landscape development (stages 5–10) was severely restricted. Unit T3A for example is only preserved at a few locations owing to its relatively uncemented nature and inset position. On the basis of the extent of pedogenic overprinting of T3A relative to T4 (Oldknow, 2016), T3A appears to be considerably older than T4, which apparently was deposited in the late Holocene (Section 5.1) and is the best preserved valley fill after T2. If T3B at Wilgerbosch reflected the remains of a catchment-wide rather than local-fill terrace, this implies that additional 'cut and fill' cycles may have occurred between stages 7 and 10; but because of preservation factors, the stratigraphic evidence has been removed.

Negligible rates of tectonic uplift in the Sneeuberg since the mid-Pleistocene have not been conducive to the preservation of valley fills of the age found in many basins across the Mediterranean (Hattingh, 1996; Macklin et al., 2012). Rates of landscape denudation have been low enough that epeirogenic uplift caused by crustal unloading has been negligible (Decker et al., 2011, 2013). Instead, alluvial preservation in the Wilgerbosch catchment has been spatially and temporally biased most likely by (i) indirect and direct lithological controls on base-level change (Tooth et al., 2004); (ii) the intrinsic properties of soil and sediment (Rienks et al., 2000); (iii) the thickness, spatial extent, and longevity of blankets (Fryirs et al., 2007); and (iv) to a lesser extent, tributary impoundment by pockets of intact valley fill in wider reaches (Brierley and Fryirs, 1999).

5.4.5. Land use change

The drivers and timing of the most recent incision phase (stage 11) evident across the Sneeuberg have been rigorously debated (Neville, 1996; Rowntree et al., 2004). The current consensus favours an anthropogenic driver, namely the European incursion of the late eighteenth century, with unsustainable land use practices leading to incision of valley floors. For example, Neville (1996) reported that the Klein Seekoi River was characterised by chains of pools with discontinuous, low energy channels through wetland systems prior to incision. Beinart (2003) attributed loss of grass and invasion of shrubs around Graaff-Reinet (1810–1830 CE) to overgrazing by sheep. Skead (2007) reported that all major rivers of the Eastern Cape contained hippopotami when European settlers first arrived and quotes an example of wetlands (vleis) having been intentionally drained for agriculture near Somerset East in the 1830s. In addition to overgrazing, Neville et al. (1994) implicated wagon roads and tracks associated with the Kimberley diamond rush of the 1870s as a major factor contributing to vegetation degradation. Rowntree (2013) analysed several earlier writings about 'the evil of sluits' (linear gullies) at the turn of the twentieth century and demonstrated that erosion did not begin in the Sneeuberg until after 1820 but that gullies had been incised by 1870. Boardman (2014) similarly concluded that incision of the Klein Seekoi likely occurred between 1850 and 1950. However, elsewhere in South Africa an earlier incision phase has been linked to abrupt late Holocene climate changes (Lyons et al., 2013) rather than an anthropogenic driver as demonstrated in the Sneeuberg. In the context of the stratigraphic legacy of 'cut and fill' presented in this paper, the stage 11 incision phase remains unprecedented in terms of its depth and spatial extent.

6. Conclusion

Extensive alluvial exposures in the Wilgerbosch catchment have permitted the most detailed investigation yet into the characteristics, mechanisms, and drivers of terrace genesis in the Sneeuberg, an area located in a transitional climatic zone of South Africa.

The continuity of four major fills that are sedimentologically, stratigraphically, and magnetically distinct across the catchment is evidence of regional changes in the sediment- to-discharge ratio rather than individual reaches. Preliminary OSL dating evidence indicates that the oldest deposits are at least post-LGM in age but may well be LGM or older in the higher order channels. Having ruled out rock barrier breach, tectonic, and eustatic influences, complex interactions between periglaciation and fluvial activity emerges as the most important control on cut, fill, and pedogenesis in the early part of the terrace record. A series of complex responses to this earlier phase involving blanket genesis is shown to decrease alluvial storage capacity, such that the terrace record appears to be spatially and temporally biased toward the late Pleistocene and late Holocene terraces (1–2 and 4 respectively). A secondary effect of this biasing is that barrier modification and incision by fluvial activity is highly episodic, but subsurface weathering is important for priming barriers to incision during periods when channel cutting exceeds terrace thickness. The multitude of geological barriers that appear to have been incised prior to late Pleistocene terrace formation may have sensitised the catchment to allogenic drivers such that 'cut and fill' features exceed the scale and complexity of those on the northward side of the Sneeuberg. Evidence of recent dolerite barrier breach in the catchment headwaters means that reaches formerly prone to localised autogenic 'cut and fill' have become sensitised to catchment-wide geomorphic adjustments. The most recent incision phase appears to be unprecedented in terms of its depth and extent compared to previous phases of channel entrenchment.

Further research can test and apply alternative dating methods to quartz-OSL and ^{14}C to calculate terrace aggradation rates, test extent of synchronicity within and between terraces, and compare against other regional geoproxy and palaeoclimatic records. The results of this study likely have wider implications for interpreting and understanding landscape response in morphologically similar headwater valleys in the Great Karoo, South Africa, and other global semiarid landscapes.

Acknowledgements

This doctoral research was funded by the Natural Environmental Research Council (1093015). The authors wish to thank: Prof. Kate Rowntree of Rhodes University for providing aerial photographs of the study region and lending us field equipment; Prof. Frank Oldfield for guidance in conducting magnetics measurements and interpretation of results; Prof. Andreas Lang, Dr. Barbara Mauz, and Mrs. Susan Packman for advice regarding the sampling methodology and interpretation of OSL results; Prof. Stephen Tooth and Dr. James Cooper for examining and commenting in detail on the sedimentological and stratigraphic aspects of this study; the three anonymous reviewers for their constructive remarks that helped us to clarify some aspects of the methods, analyses, and interpretations; and Hester and JP of Ganora farm, South Africa, for generously giving us permission to work on their land.

Appendix A

Table A.1
Sedimentary characteristics of the major valley fills (superscripted numbers refer to distinct facies associations).

Terrace	Log/unit	Morphology	Summary description	Interpretation
1	[1]AK-5/A-B [1]AK-6/A [1]AK-7/A [1]AK-9/A-C [1]AK-10/A [1]AK-11/A [1]AK-12/A [2*]GG-S [2]GG-2/B	Valley margin terrace. Most complete preservation in gorge and colluvial depressions in valley headwaters. Thickness: 0.4–5 m.	[1]Altered massive or thin-medium horizontally-bedded sands (Sm) or bioturbated clayey silts (Fr). Gravels may be massive (Gm) or horizontally bedded (Gmh). [2]Altered diamicton (Dmm) and clast-supported gravels (Gh).	[1]Fine-grained slopewash deposits. [2]Head (gelifluction) and slopewash deposits.
2	[1]AK-7/B-Q [2]AK-8/A-B [2]AK-9/D-K [2]AK-15/A-B [3]AK-10/B [3]AK-11/B-E [3]AK-12/B	Typically overlaps or is inset within T1 on both banks. In cases where has been T1 stripped, T2 overlies bedrock. Thickness: 1.8–6.2 m.	[1]Altered matrix-supported gravels with horizontal or planar cross-bedding (Gmh and Gp), and sands which are either massive or exhibit planar cross bedding (Sm and Sp) [2]Altered thick beds (up to 0.95 m) of matrix or clast-supported gravels (Gmh or Gh) and cobbles (Cmm) with basal unconformities. [3]Successions of matrix-supported gravels (Gmh or Gmm) or	[1]Infilled palaeogully. [2]Debris flow deposits sourced from nearby dolerite slopes. [3]Channel deposits including: medial bars, dunes (2D and 3D) and debris flows. Overbank deposits reflected in

(continued on next page)

Table A.1 (*continued*)

Terrace	Log/unit	Morphology	Summary description	Interpretation
	[3]AK-13/A-C [3]AK-14/A-J [3]GG-1/A-C [3]GG-2/A [3]WGR-3/A-E [3]WGK-4/A [3]WGK-5/A-D [3]WGK-6/A-C		imbricated gravels (Gh), cobbles (Ch) or boulders (B), interspersed by sand units (Sm) of varying thickness (0.1–1.5 m) or silty sand (Fsm). Sands may exhibit planar (Sp) or trough cross bedding (St).	silty sands.
3A	AK-11/F-G AK-12/C AK-14/K AK-15/C-I GG-1/D-F	Overlaps and is inset within T2. Thickness ranges from 0.3–3.3 m.	Altered beds of matrix (Gmh/Gmm) or clast-supported gravel (Gh), sand (Sm/Sh) and silt (Fsm). Some units exhibit inverse grading. Planar and trough cross bedding may be present (Sp & St).	Medial bar, debris flow and channel sediments (2D and 3D dunes) deposited in a migrating channel.
3B	[1]WGK-7/A [2]WGK-8/A-B	Restricted to lower WGK valley. Thickness: 2–3 m.	Slightly altered deposits of sand (Sm) and matrix-supported gravel (Gmh).	[1]Slopewash deposits. [2]Channel bedload and bar deposits.
4	[1]AK-8/C [1]AK-10/C [1]AK-13/D-F [1]WGK-5/E [1]WGK-6/D [1]WGK-9/A2 [2]AK-8/D-E [2]AK-9/L [2]AK-10/D [2]AK-13/G [2]WGK-4/B [2]WGK-6/E [3]AK-16/A, C, E [3]WGR-1/C, E [3]WGR-2/A, C, E, H [3]WGR-3/G, L [3]WGR-4/C [4]AK-16/B, D, F-I [4]WGK-9/B [4]WGR-1/A, B, D, F [4]WGR-2/B, D, F, G, I [4]WGR-3/F, H, I, K, M, N	Inset within T2 and T3. Thickness ranges from 0.95–4.2 m.	[1]Gleyed units of silty sand (Fsm/Fr) or sandy silt (Sm/Fl) which lack plant fossils. [2]Unaltered, thickly laminated sands (Tl) or silt (Fm). [3]Sandy silt or silty sand units which may contain fossil bivalve shells and/or plant macrofossils (Frc). [4]Non-gleyed clastic units of matrix or clast-supported gravels (Gmh or Gh), sands (Sm) and/or silts (Fsm). Coarser units may exhibit inverse grading and vary in thickness (0.1-1 m).	[1]Low energy wetland channel with near surface water table. [2]Overbank deposits. [3]Low energy wetland channel [4]Channel lag deposits emplaced during floods.

Table A.2
Magnetic susceptibility and Coulter grain size data for discontinuous valley fills.

Terrace	Outcrop/unit	Height (m)	X_{LF} (10^{-8} m^3 kg^{-1})	D_{10} (μm)	D_{50} (μm)	D_{90} (μm)	Textural group
AKH-A	AK-1/A1	0.40	162	004	0313	1354	Sandy silt
	AK-1/A1	0.60	070	009	1007	1616	Sandy silt
	AK-1/A2	0.75	164	005	0261	1338	Sandy silt
AKH-B	AK-1/B2	1.10	160	011	0785	1605	Sandy silt
	AK-1/B2	1.20	076	005	0696	1525	Sandy silt
	AK-1/B3	2.00	147	006	0860	1573	Sandy silt
	AK-2/A	0.10	089	–	–	–	Sandy silt
	AK-2/E1	0.80	087	–	–	–	Sandy silt
	AK-3/A1	0.25	080	003	0019	0132	Silty sand
	AK-3/A1	0.60	088	005	0549	1372	Sandy silt
	AK-3/A2	0.90	106	224	0907	1426	Sand
	AK-4/B	0.30	088	013	0768	1689	Sandy silt
AKH-C	AK-2/F1	1.75	150	–	–	–	Sandy silt
	AK-3/B	1.65	144	004	0044	1218	Silty sand
	AK-4/E	1.40	143	002	0010	0050	Silty clay
AKH-D	AK-4/F2	2.05	146	492	1184	1788	Sand
	AK-4 palaeogully	–	120	–	–	–	Sand
WGK-A	WGK-2/A1	0.20	036	224	0948	1646	Sand
	WGK-2/A2	0.40	034	005	0727	1510	Sandy silt
	WGK-3/A2	0.55	029	003	1080	1661	Sandy silt
	WGK-3/B2	1.10	049	012	0142	1120	Sandy silt
	WGK-3/C	1.50	040	550	1155	1705	Sand
	WGK-3/D	2.00	035	257	0855	1562	Sand
	WGK-3/E	2.40	042	013	0878	1569	Sandy silt
WGK-B	WGK-1/A1	0.10	057	007	0728	1600	Sandy silt

Table A.2 (*continued*)

Terrace	Outcrop/unit	Height (m)	X_{LF} (10^{-8} m^3 kg^{-1})	D_{10} (μm)	D_{50} (μm)	D_{90} (μm)	Textural group
	WGK-1/A2	0.40	053	008	0932	1599	Sandy silt
	WGK-1/A3	0.65	058	026	1049	1733	Sand
	WGK-1/A4	0.90	054	002	0066	0945	Sandy silt
	WGK-1/A5	1.10	059	012	0975	1760	Sandy silt
	WGK-1/A6	1.20	040	164	1007	1654	Sand
	WGK-1/A6	1.40	056	003	0477	1416	Sandy silt
	WGK-1/A7	1.70	047	167	0709	1568	Sand
	WGK-2/C	1.70	059	009	0580	1309	Sandy silt
	WGK-2/C	1.95	055	004	0500	1451	Sandy silt
Unclassified	[4]WGR-4/A	0.30	042	021	0187	0466	Sandy silt
	[4]WGR-4/B1	0.55	036	004	0066	0164	Sandy silt
	[4]WGR-4/B2	3.40	027	002	0007	0046	Clayey silt

Table A.3
Magnetic susceptibility and Coulter grain size data for Terrace 1.

Outcrop/unit	Height (m)	X_{LF} (10^{-8} m^3 kg^{-1})	D_{10} (μm)	D_{50} (μm)	D_{90} (μm)	Textural group
Terrace 1						
[1]AK-5/B1	0.60	024	02	0010	0151	Silty sand
[1]AK-5/B2	1.65	070	44	6071	1649	Sandy silt
[1]AK-6/A	0.25	112	02	0011	0118	Silty sand
[1]AK-6/B	0.70	099	44	1159	1816	Sandy silt
[1]AK-9/B	0.20	059	13	0256	1491	Sandy silt
[1]AK-9/C2	0.60	069	34	0517	1509	Sandy silt
[1]AK-10/A2	1.05	024	05	0130	1555	Sandy silt
[1]AK-11/A	0.30	028	03	0111	1321	Sandy silt
[1]AK-12/A1	0.45	037	06	0060	1513	Silty sand
[2]*GG-S*	1.50	056	02	0038	0940	Silty sand

Table A.4
Magnetic susceptibility and Coulter grain size data for Terrace 2.

Outcrop/unit	Height (m)	X_{LF} (10^{-8} m^3 kg^{-1})	D_{10}(μm)	D_{50}(μm)	D_{90}(μm)	Textural group
Terrace 2						
[1]AK-7/B	0.30	087	050	0939	1700	Sandy silt
[1]AK-7/E	0.90	087	019	0584	1681	Sandy silt
[2]AK-8/B	0.70	091	–	–	–	Sand
[2]AK-9/F	1.90	092	007	0109	0438	Sandy silt
[2]AK-9/H	2.30	099	010	0139	1232	Sandy silt
[2]AK-9/J	2.80	111	010	0076	0730	Sandy silt
[2]AK-15/B	2.20	087	010	0386	1159	Sandy silt
[3]AK-11/E2	2.00	080	011	0094	1005	Sandy silt
[3]AK-12/B3	1.60	062	011	0164	1647	Sandy silt
[3]AK-12/B3	2.00	068	–	–	–	–
[3]AK-12/B3	2.25	052	005	0079	0691	Sandy silt
[3]AK-13/A	0.10	050	029	0680	1607	Sandy silt
[3]AK-13/B2	0.60	062	012	0142	1120	Sandy silt
[3]AK-14/A	0.40	068	017	1045	1743	Sandy silt
[3]AK-14/D	1.90	066	008	0268	1212	Sandy silt
[3]AK-14/H	3.20	042	007	0110	1404	Sandy silt
[3]AK-14/J	4.70	056	022	0841	1626	Sandy silt
[3]WGK-4/A	1.30	053	003	0449	1451	Sandy silt
[3]WGK-4/A	1.75	069	003	0483	1271	Sandy silt
[3]WGK-5/C	0.60	048	003	0059	0547	Silty sand
[3]WGK-5/D1	1.30	037	406	0983	1505	Sand
[3]WGK-5/D1	1.80	064	029	0841	1541	Sandy silt
[3]WGK-6/A3	0.70	028	003	0150	1560	Sandy silt
[3]WGK-6/C3	1.95	038	339	0973	1510	Sand
[3]WGR-3/B	0.75	034	095	0752	1609	Sand
[3]WGR-3/E	2.30	042	003	0071	0557	Sandy silt
[3]GG-1/B	1.10	040	002	0019	0240	Silty clay

Table A.5
Magnetic susceptibility and Coulter grain size data for Terraces 3A and 3B.

Outcrop/unit	Height (m)	X_{LF} (10^{-8} m^3 kg^{-1})	D_{10}(μm)	D_{50}(μm)	D_{90}(μm)	Textural group
Terrace 3A						
AK-11/F1	2.85	34	006	0059	0872	Silty sand
AK-11/F2	4.25	62	011	0285	1381	Sandy silt
AK-12/C	3.95	95	009	0081	1325	Sandy silt

(*continued on next page*)

Table A.5 (*continued*)

Outcrop/unit	Height (m)	X_{LF} (10^{-8} m^3 kg^{-1})	D_{10}(μm)	D_{50}(μm)	D_{90}(μm)	Textural group
AK-15/C	3.00	65	337	1040	1756	Sand
GG-1/D2	2.90	43	012	1064	1725	Sandy silt
GG-1/D3	3.75	42	014	0903	1737	Sandy silt
Terrace 3B						
[1]WGK-7/A1	0.30	49	004	0135	1389	Sandy silt
[1]WGK-7/A2	1.00	41	002	0144	1443	Sandy silt
[1]WGK-7/A5	1.75	36	014	0422	1622	Sandy silt
[2]WGK-8/A1	0.20	37	005	0111	0666	Sandy silt
[2]WGK-8/A3	0.75	39	016	0259	0720	Sandy silt
[2]WGK-8/B2	1.70	36	003	0126	0843	Sandy silt

Table A.6
Magnetic susceptibility and Coulter grain size data for Terrace 4.

Outcrop/unit	Height (m)	X_{LF} (10^{-8} m^3 kg^{-1})	D_{10}(μm)	D_{50}(μm)	D_{90}(μm)	Textural group
Terrace 4						
[1]AK-8/C1	2.00	51	004	0052	1092	Silty sand
[1]AK-10/C	3.80	29	003	0750	1565	Sandy silt
[1]AK-13/D	1.75	28	004	0026	0177	Silty sand
[1]AK-13/E	3.10	16	005	0050	0199	Silty sand
[1]AK-13/F	4.40	25	006	0065	0770	Sandy silt
[1]WGK-5/E	2.60	31	009	0638	1582	Sandy silt
[1]WGK-6/D	3.00	16	001	0004	0018	Clayey silt
[1]WGK-9/A2	1.50	12	001	0005	0033	Clayey silt
[2]AK-8/D	3.65	63	007	0999	1705	Sandy silt
[2]AK-10/D	4.80	61	005	1061	1754	Sandy silt
[2]WGK-4/B1	2.00	49	020	0185	0999	Sandy silt
[2]WGK-6/E	3.50	38	047	0633	1414	Sandy silt
[3]AK-16/A	1.05	–	003	0035	0266	Silty sand
[3]AK-16/C	1.45	75	003	0092	1238	Sandy silt
[3]AK-16/C	1.60	71	004	0102	1431	Sandy silt
[3]AK-16/E	1.85	45	003	0073	1160	Sandy silt
[3]WGR-1/E	1.05	19	005	0065	0608	Sandy silt
[3]WGR-2/A	0.40	18	003	0140	0796	Sandy silt
[3]WGR-2/C	0.90	22	004	0216	1050	Sandy silt
[3]WGR-2/E	1.40	32	001	0005	0027	Silty clay
[3]WGR-2/H1	2.70	21	003	0069	0142	Sandy silt
[3]WGR-2/H3	3.20	24	012	0142	1120	Sandy silt
[3]WGR-3/G	4.50	11	002	0009	0039	Silty clay
[3]WGR-3/L	5.65	22	003	0029	0173	Silty sand
[4]WGR-4/C2	4.05	16	003	0058	0188	Silty sand
[4]WGK-9/B1	2.25	13	002	0009	0947	Silty sand
[4]WGR-1/D1	0.80	27	311	0848	1431	Sand
[4]WGR-2/F	1.70	24	014	0688	1275	Sandy silt
[4]WGR-3/F1	3.25	23	214	0955	1625	Sand

References

Adamiec, G., Aitken, M., 1998. Dose-rate conversion factors: update. Ancient TL 16:37–50. http://dx.doi.org/10.1016/S0277-3791(03)00021-0.

Arnold, L.J., Bailey, R.M., Tucker, G.E., 2007. Statistical treatment of fluvial dose distributions from southern Colorado arroyo deposits. Quat. Geochronol. 2 (1–4), 162–167.

Balling, R.C., Wells, S.G., 1990. Historical rainfall patterns and arroyo activity within the Zuni River drainage basin, New Mexico. Ann. Assoc. Am. Geogr. 80 (4), 603–617.

Beinart, W., 2003. The Rise of Conservation in South Africa: Settlers, Livestock and the. Environment 1770–1950. Oxford University Press, Oxford.

Benedict, J.B., 1976. Frost creep and gelifluction features: a review. Quat. Res. 6, 55–76.

Blott, S.J., Pye, K., 2001. GRADISTAT: a grain size distribution and statistics package for the analysis of unconsolidated sediments. Earth Surf. Process. Landf. 26 (11), 1237–1248.

Boardman, J., 2014. How old are the gullies (dongas) of the Sneeuberg uplands, Eastern Karoo, South Africa? Catena 113, 79–85.

Boardman, J., Parsons, A.J., Holland, R., Holmes, P.J., Washington, R., 2003. Development of badlands and gullies in the Sneeuberg, Great Karoo, South Africa. Catena 50 (2–4), 165–184.

Boardman, J., Holmes, P.J., Rhodes, E.J., Bateman, M.D., 2005. Colluvial fan gravels, depositional environments and luminescence dating: a Karoo case study. S. Afr. Geogr. J. 87 (1), 73–79.

Boardman, J., Foster, I., Rowntree, K., Mighall, T.M., Gates, J.B., 2010. Environmental stress and landscape recovery in a semi-arid area, the Karoo, South Africa. Scott. Geogr. J. 126 (2), 64–75.

Born, S.M., Ritter, D.F., 1970. Modern terrace development near Pyramid Lake Nevada, and its geologic implications. Geol. Soc. Am. Bull. 81 (4), 1233–1242.

Botha, G.A., Fedoroff, N., 1995. Palaeosols in late quaternary colluvium, northern KwaZulu-Natal, South Africa. J. Afr. Earth Sci. 21 (2), 291–311.

Botha, G.A., Wintle, A.G., Vogel, J.C., 1994. Episodic late quaternary palaeogully erosion in northern KwaZulu-Natal, South Africa. Catena 23 (3–4), 327–340.

Bousman, C.B., Partridge, P.C., Scott, L., Metcalfe, S.E., Vogel, J.C., Seaman, M., Brink, J.S., 1988. Palaeoenvironmental implications of late Pleistocene and Holocene valley fills in Blydefontein Basin, Noupoort, C.P. South Africa. Palaeontol. Afr. 19, 43–67.

Bridgland, D., Westaway, R., 2008. Climatically controlled river terrace staircases: a worldwide quaternary phenomenon. Geomorphology 98 (3–4), 285–315.

Brierley, G.J., Fryirs, K., 1999. Tributary-trunk stream relations in a cut and fill landscape: a case study from Wolumla catchment, New South Wales, Australia. Geomorphology 28 (1–2), 61–73.

Bull, W.B., 1972. Recognition of alluvial fan deposits in the stratigraphic record. In: Hamblin, W.K., Rigby, J.K. (Eds.), Recognition of Ancient Sedimentary Environments. Society of Economic Palaeontologists and Mineralogists Special Publication 16, pp. 63–83.

Bull, W.B., 1991. Geomorphic Responses to Climate Change. Oxford University Press, New York, p. 326.

Butzer, K.W., 1984. Late quaternary environments in South Africa. In: Vogel, J.C. (Ed.), Late Quaternary Palaeoclimates of the Southern Hemisphere. Balkema, Rotterdam, pp. 235–264.

Butzer, K.W., Helgren, D.M., Fock, G.J., Stuckenrath, R., 1973. Alluvial terraces of the lower Vaal River, South Africa: a reappraisal and reinvestigation. J. Geol. 81 (3), 341–362.

Candy, I., Black, S., 2009. The timing of quaternary calcrete development in semi-arid southeast Spain: investigating the role of climate on calcrete genesis. Sediment. Geol. 218 (1–4), 6–15.

Cantuneanu, O., Wopfner, H., Eriksson, P.G., Cairncross, B., Rubidge, B.S., Smith, R.M.H., Hancox, P.J., 2005. The Karoo basins of south-central Africa. J. Afr. Earth Sci. 43 (1–3), 211–253.

Chase, B.M., Meadows, M.E., 2007. Late quaternary dynamics of southern Africa's winter rainfall zone. Earth-Sci. Rev. 84 (3–4), 103–138.
Chase, B.M., Boom, A., Carr, A.S., Carré, M., Chevalier, M., Meadows, M.E., Pedro, J.B., Stager, J.C., Reimer, P.J., 2015a. Evolving southwest African response to abrupt deglacial North Atlantic climate change events. Quat. Sci. Rev. 121, 132–136.
Chase, B.M., Lim, S., Chevalier, M., Boom, A., Carr, A.S., Meadows, M.E., Reimer, P.J., 2015b. Influence of tropical easterlies in southern Africa's winter rainfall zone during the Holocene. Quat. Sci. Rev. 107, 138–148.
Cheetham, M.D., Bush, R.T., Keene, A.F., Erskine, W.D., 2010. Nonsynchronous, episodic incision: evidence of threshold exceedance and complex response as controls terrace formation. Geomorphology 123 (3–4), 320–329.
Clarke, M.L., Vogel, J.C., Botha, G.A., Wintle, A.G., 2003. Late quaternary hillslope evolution recorded in eastern South African colluvial badlands. Palaeogeogr. Palaeoclimatol. Palaeoecol. 197 (3–4), 199–212.
Damm, B., Hagedorn, J., 2010. Holocene floodplain formation in the southern Cape region, South Africa. Geomorphology 122, 213–222.
Decker, J.E., Niedermann, S., de Wit, M.J., 2011. Soil erosion rates in South Africa compared with cosmogenic 3 He-based rates of soil production. S. Afr. J. Geol. 114, 475–488.
Decker, J.E., Niedermann, S., de Wit, M.J., 2013. Climatically influenced denudation rates of the southern African plateau: clues to solving a geomorphic paradox. Geomorphology 190, 48–60.
Duller, G.A.T., 2003. Distinguishing quartz and feldspar in single grain luminescence measurements. Radiat. Meas. 37 (2), 161–165.
Erkens, G., Dambeck, R., Volleberg, K.P., Bouman, M.T.I.J., Bos, J.A.A., Cohen, K.M., Wallinga, J., Hoek, W.Z., 2009. Fluvial terrace formation in the northern Upper Rhine Graben during the last 20,000 years as a result of allogenic controls and autogenic evolution. Geomorphology 103 (3), 476–495.
Foster, I.D.L., Rowntree, K.M., 2012. Sediment yield changes in the semi-arid Karoo: a palaeoenvironmental reconstruction of sediments accumulating in Cranemere Reservoir, Eastern Cape, South Africa. Z. Geomorphol. 56 (3), 131–146.
Foster, I.D.L., Boardman, J., Keay-Bright, J., 2007. Sediment tracing and environmental history for two small catchments, Karoo Uplands, South Africa. Geomorphology 90 (1–2), 126–143.
Fryirs, K., 2013. (Dis)Connectivity in catchment sediment cascades: a fresh look at the sediment delivery problem. Earth Surf. Process. Landf. 38 (1), 30–46.
Fryirs, K., Brierley, G.J., 2010. Antecedent controls on river character and behaviour in partly-confined valley settings: upper Hunter catchment, NSW, Australia. Geomorphology 117, 106–120.
Fryirs, K., Brierley, G.J., Preston, N.J., Kasai, M., 2007. Buffers, barriers and blankets: the (dis)connectivity of catchment-scale sediment cascades. Catena 70 (1), 49–67.
Gil García, M.J., Dorado Valiño, M., Valdeolmillos Rodríguez, A., Ruiz-Zapata, M.B., 2002. Late-glacial and Holocene palaeoclimatic record from Sierra de Cebllorea (northern Iberian range, Spain). Quat. Int. 93-94, 13–18.
González-Amuchastegui, M.J., Serrano, E., 2013. Acumulaciones tobáceas y evolución del paisaje: cronología y fasas morfogenéticas en al Alto Ebro (Burgos). Cuaternario Geomorfol. 27, 9–32.
Grenfell, M.C., Ellery, W., Grenfell, S.E., 2009. Valley morphology and sediment cascades within a wetland system in the KwaZulu-Natal Drakensberg Foothills, Eastern South Africa. Catena 78 (1), 20–35.
Grenfell, S.E., Rowntree, K.M., Grenfell, M.C., 2012. Morphodynamics of a guly and floodout system in the Sneeuberg Mountains of the semi-arid Karoo, South Africa: implications for local landscape connectivity. Catena 89 (1), 8–21.
Grenfell, S.E., Grenfell, M.C., Rowntree, K.M., Ellery, W.N., 2014. Fluvial connectivity and climate: a comparison of channel pattern and process in two climatically contrasting fluvial sedimentary systems in South Africa. Geomorphology 205, 142–154.
Hanvey, P.M., Lewis, C.A., 1990. A preliminary report on the age and significance of quaternary lacustrine deposits at Birnam, north-east Cape Province, South Africa. S. Afr. J. Sci. 86, 271–273.
Harden, T., Macklin, M.G., Baker, V.R., 2010. Holocene flood histories in south-western USA. Earth Surf. Process. Landf. 35 (6), 707–716.
Harvey, J.E., Pederson, J.L., Rittenour, T.M., 2011. Exploring relations between arroyo cycles and canyon palaeoflood records in Buckskin Wash, Utah: reconciling scientific paradigms. Geol. Soc. Am. Bull. 123 (11—12), 2266–2276.
Hattingh J. 1996. 'Fluvial response to allocyclic influences during the development of the lower Sundays River, Eastern Cape, South Africa.' Quat. Int. 33 (0), pp. 3–10.
Hattingh, J., Rust, I.C., 1999. Drainage evolution of the Sundays River, South Africa. In: Miller, A., Gupta, A. (Eds.), Varieties in Fluvial Form. John Wiley and Sons, Chichester, pp. 145–166.
Hereford, R., 1986. Modern alluvial history of the Paria River drainage basin, southern Utah. Quat. Res. 25 (3), 293–311.
Hereford, R., Webb, R., 1992. Historic variation of warm-season rainfall, southern Colorado plateau, southwestern USA. Clim. Chang. 22 (3), 239–256.
Hogg, A.G., Hua, Q., Blackwell, P.G., Niu, M., Buck, C.E., Guilderson, T.P., Heaton, T.J., Palmer, J.G., Reimer, P.J., Reimer, R.W., Turney, C.S.M., Zimmerman, S.R.H., 2013. SHCal13 southern hemisphere calibration, 0–50,000 years cal BP. Radiocarbon 51 (4), 1165–1176.
Holmes, P.J., 2001. Central Great Karoo headwater catchments and valley fills; an overview of short term change. S. Afr. Geogr. J. 83 (3), 274–282.
Holmes, P.J., Boardman, J., Parsons, A.J., Marker, M.E., 2003. Geomorphological palaeoenvironments of the Sneeuberg Range, Great Karoo, South Africa. J. Quat. Sci. 18 (8), 801–813.
Hooke, J., 2003. Coarse sediment connectivity in river channel systems: a conceptual framework and methodology. Geomorphology 56 (1–2), 79–94.
Hooke, J., 2004. Analysis of coarse sediment connectivity in a semiarid river channel. In: Golosov, V., Belyaev, V., Walling, D.E. (Eds.), Sediment Transfer through the Fluvial System, ICCE Moscow, August 2004. 288. Wallingford International Association of the Hydrological Sciences, pp. 269–275.
Horton, R.E., 1945. Erosional development of streams and their drainage basins: Hydrophysical approach to quantitative morphology. Bull. Geol. Soc. Am. 56, 275–370.
Houben, P., 2003. Spatio-temporally variable response of fluvial systems to Late Pleistocene climate change: a case study from central Germany. Quat. Sci. Rev. 22, 2125–2140.
Inman, D.L., Jenkins, S.A., 1999. Climate change and the episodicity of sediment flux of small California rivers. J. Geol. 107, 251–270.
Jones, L.S., Rosenburg, M., del Mar, Figueroa M., McKee, K., Haravitch, B., Hunter, J., 2010. Holocene valley-floor deposition and incision in a small drainage basin in western Colorado, USA. Quat. Res. 74 (2), 199–206.
Keen-Zebert, A., Tooth, S., Rodnight, H., Duller, G.A.T., Roberts, H.M., Grenfell, M., 2013. Late quaternary floodplain reworking and the preservation of alluvial sedimentary archives in unconfined and confined river valleys in the eastern interior of South Africa. Geomorphology 185 (0), 54–66.
Kemp, R.A., 1985. The decalcified Lower Loam at Swanscombe, Kent: a buried Quaternary soil. Proc. Geol. Assoc. 96 (4), 343–355.
Klappa, C.F., 1980. Brecciation textures and tepee structures in quaternary calcrete (caliche) profiles from eastern Spain: the plant factor in their formation. Geol. J. 15 (2), 81–89.
Knox, J.C., 1972. Valley alluviation in southwestern Wisconsin. Ann. Assoc. Am. Geogr. 62 (3), 401–410.
Knox, J.C., 1993. Large increases in flood magnitude in response to modest changes in climate. Nature 361 (6411), 430–432.
Leopold, L.B., Wolman, M.G., Miller, J.P., 1964. Fluvial Processes in Geomorphology. W.H. Freeman and Company, San Francisco, CA, p. 522.
Lewin, J., Macklin, M.G., 2003. Preservation potential for late quaternary river alluvium. J. Quat. Sci. 18 (2), 107–120.
Lewis, C.A., 1999. Field Guide to the Quaternary in the Eastern and Southern Cape, South Africa. Rhodes University, Grahamstown, p. 79.
Lewis, C.A., 2005. Late Glacial and Holocene palaeoclimatology of the Drakensberg of the Eastern Cape, South Africa. Quat. Int. 129, 33–48.
Lewis, C.A., 2008. Late quaternary climatic changes, and associated human responses, during the last similar to 45000 yr in the Eastern and adjoining Western Cape, South Africa. Earth-Sci. Rev. 88 (3–4), 167–187.
Love, D.W., 1977. Dynamics of sedimentation and geomorphic history of Chaco Canyon National Monument, New Mexico. New Mexico Geological Society, Guidebook to 28th Field Conference, pp. 291–300.
Lyons, R., Tooth, S., Duller, G.A., 2013. Chronology and controls of donga (gully) formation in the upper Blood River catchment, KwaZulu-Natal, South Africa: evidence for a climatic driver of erosion. The Holocene 23 (12), 1875–1887.
Lyons, R., Tooth, S., Duller, G.A., 2014. Late quaternary climatic changes revealed by luminescence dating, mineral magnetism and diffuse reflectance spectroscopy of river terrace palaeosols: a new form of geoproxy data for the southern African interior. Quat. Sci. Rev. 95, 43–59.
Macklin, M.G., Fuller, I.C., Lewin, J., Maas, G.S., Passmore, D.G., Rose, J., Woodward, J.C., Black, S., Hamlin, R.H.G., Rowan, J.S., 2002. Correlation of fluvial sequences in the Mediterranean basin over the last 200 ka and their relationship to climate change. Quat. Sci. Rev. 21, 1633–1641.
Macklin, M.G., Lewin, J., Woodward, J.C., 2012. The fluvial record of climate change. Philos. Trans. R. Soc. 370, 2143–2172.
Marker, M.E., 1995. Late quaternary environmental implications from sedimentary sequences at 2 high-altitude Lesotho sites. S. Afr. J. Sci. 91 (6), 294–298.
McFadden, L.D., McAuliffe, J.R., 1997. Lithologically influenced geomorphic responses to Holocene climatic changes in the Southern Colorado Plateau, Arizona: a soil-geomorphic and ecologic perspective. Geomorphology 19 (3–4), 303–332.
Merritts, D.J., Vincent, K.R., Wohl, E.E., 1994. Long river profiles, tectonism, and eustasy: a guide to interpreting fluvial terraces. J. Geophys. Res. Solid Earth 99 (B7), 14031–14050.
Miall, A.D., 1996. The Geology of Fluvial Deposits: Sedimentary Facies, Basin Analysis and Petroleum Geology. Springer-Verlag, Berlin, p. 79.
Molnar, P., 2004. Late Cenozoic increase in accumulation rate of terrestrial sediment: how might climate change have affected erosion rates? Annu. Rev. Earth Planet. Sci. 32, 67–89.
Montgomery, D.R., Dietrich, W.E., 1992. Channel initiation and the problem of landscape scale. Science 255, 826–830.
Mucina, L., Rutherford, M.C., Palmer, A.R., Milton, S.J., Scott, L., Wendy-Lloyd, J., van der Merwe, B., Hoare, D.B., Bezuidenhout, H., Vlok, J.H.J., Euston-Brown, D.I.W., Powrie, L.W., Dold, A.P., 2006. Nama-Karoo biome. In: Mucina, L., Rutherford, M.C. (Eds.), The Vegetation of South Africa, Lesotho and Swaziland. South African National Botanical Institute, Pretoria, pp. 324–347.
Murray, A.S., Wintle, A.G., 2000. Luminescence dating of quartz using an improved single-aliquot regenerative-dose protocol. Radiat. Meas. 32 (1), 57–73.
Neumann, E.R., Svensen, H., Galerne, C.Y., Planke, S., 2011. Multistage evolution of dolerites in the Karoo large igneous province, central South Africa. J. Petrol. 52 (5), 959–984.
Neville, D., 1996. European Impacts on the Seacow River Valley and its Hunter-Gatherer Inhabitants, AD 1770-1990. (Unpublished MA dissertation). University of Cape Town Part 1: pp. 281. Part 2: pp.63.
Neville, D., Sampson, B.E., Sampson, C.G., 1994. The frontier wagon track system in the Seacow River valleys, north-eastern Cape. South African Archaeological Bulletin 49, 65–72.
Nicholas, A.P., Ashworth, P.J., Kirkby, M.J., Macklin, M.G., Murray, T., 1995. Sediment slugs: large-scale fluctuations in fluvial sediment transport rates and storage volumes. Prog. Phys. Geogr. 19 (4), 500–519.
Nichols, G.J., Fisher, J.A., 2007. Processes, facies and architecture of fluvial distributary system deposits. Sediment. Geol. 195 (1–2), 75–90.

Oldknow, C.J., 2016. Late Quaternary Landscape Evolution in the Great Karoo, South Africa: Processes and Drivers. (PhD thesis). University of Liverpool, Liverpool, UK.
Osmaston, H.A., Harrison, S.P., 2005. The late quaternary glaciation of Africa: a regional synthesis. Quat. Int. 138-139, 32–54.
Partridge, T.C., Demenocal, P.B., Lorentz, S.A., Paiker, M.J., Vogel, J.C., 1997. Orbital forcing of climate over South Africa: a 200,000-year rainfall record from the Pretoria Saltpan. Quat. Sci. Rev. 16 (10), 1125–1133.
Patton, P.C., Schumm, S.A., 1981. Ephemeral-stream processes: implications for studies of quaternary valley fills. Quat. Res. 15 (1), 24–43.
Peglar, S.M., Fritz, S.C., Birks, H.J.B., 1989. Vegetation and land-use history at Diss, Norfolk. J. Ecol. 77, 203–222.
Petit, T.R., Jouzel, D., Raynaud, N.I., Barkov, N.I., Barnola, J.M., Basile, I., Bender, M., Chappellaz, J., Davis, M., Delaygue, G., Delmotte, M., Kotlyakov, V.M., Legrand, M., Lipenkov, V.Y., Lorius, C., Pépin, L., Ritz, C., Saltzman, E., Stievenard, M., 1999. Climate and atmospheric history of the past 420,000 years from the Vostok ice core, Antarctica. Nature 399, 429–436.
Reason, C.J.C., Landman, W., Tennant, W., 2006. Seasonal to decadal prediction of southern African climate and its links with variability of the Atlantic Ocean. Bull. Am. Meteorol. Soc. 87 (7), 941–955.
Renaut, R.W., 1993. Zeolitic diagenesis of late quaternary fluviolacustrine sediments and associated calcrete formation in the Lake Bogoria Basin, Kenya Rift Valley. Sedimentology 40, 271–301.
Rienks, S.M., Botha, G.A., Hughes, J.C., 2000. Some physical and chemical properties of sediments exposed in a gully (donga) in northern KwaZulu-Natal, South Africa and their relationship to the erodibility of the colluvial layers. Catena 39 (1), 11–31.
Rodnight, H., Duller, G.A.T., Wintle, A.G., Tooth, S., 2006. Assessing the reproducibility and accuracy of optical dating of fluvial deposits. Quat. Geochronol. 1 (2), 109–120.
Rose, J., Candy, I., Lee, J.R., 2000. Leet Hill (TM 384926): pre-glacial and glaciofluvial river deposits – with possible evidence for a major glaciation prior to the deposition of the Lowestoft Till. In: Lewis, S.G., Whiteman, C.A., Preece, R.C. (Eds.), The Quaternary of Norfolk and Suffolk. Quaternary Research Association, London, pp. 297–301.
Rowntree, K., 2013. The evil of sluits: a re-assessment of soil erosion in the Karoo of South Africa as portrayed in century-old sources. J. Environ. Manag. 130, 98–105.
Rowntree, K., Duma, M., Kakembo, V., Thornes, J., 2004. Debunking the myth of overgrazing and soil erosion. Land Degrad. Dev. 15, 203–214.
Rowntree, K., Foster, I., 2012. A reconstruction of historical changes in sediment sources, sediment transfer and sediment yield in a small, semi-arid Karoo catchment, South Africa. Z. Geomorphol. 56, 87–100.
Schultz, B.R., 1980. Climate of South Africa, Part 9, General Survey. Weather Bureau, Department of Transport, Pretoria.
Schumm, S.A., 1973. Geomorphic thresholds and complex response of drainage systems. Fluvial Geomorphology 6, 69–85.
Schumm, S.A., 1977. The Fluvial System. Wiley, New York, p. 338.
Schumm, S.A., 1979. Geomorphic thresholds: the concept and its applications. Trans. Inst. Br. Geogr. 4 (4), 485–515.
Sharp, R.P., Nobles, L.H., 1953. Mudflow of 1941 at Wrightwood southern California. Geol. Soc. Am. Bull. 64 (5), 547–560.
Shaw, P.A., Thomas, D.S.G., Nash, D.J., 1992. Late quaternary fluvial activity in the dry valleys (mekgacha) of the middle and southern Kalahari, southern Africa. J. Quat. Sci. 7, 273–281.
Shen, Z., Mauz, B., Lang, A., Bloemendal, J., Dearing, J., 2007. Optical dating of Holocene lake sediments: elimination of the feldspar component in fine silt quartz samples. Quat. Geochronol. 2 (1–4), 150–154.
Skead, C.J., 2007. Historical incidence of the larger land mammals in the Broader Eastern Cape. In: Boshoof, A., Kerley, G., Lloyd, P. (Eds.), Centre for African Conservation Ecology, second ed. Nelson Mandela Metropolitan University, Port Elizabeth, South Africa.
Soria-Jáuregui, A., González-Amuchastegui, M.J., Mauz, B., Lang, A., 2016. Dynamics of Mediterranean late quaternary fluvial activity: an example from the River Ebro (north Iberian Peninsula). Geomorphology 268, 110–122.
Springer, G.S., Tooth, S., Wohl, E.E., 2005. Dynamics of pothole growth as defined by field data and geometrical description. J. Geophys. Res. Earth 110, F04010.
Springer, G.S., Tooth, S., Wohl, E.E., 2006. Theoretical modelling of stream potholes based upon empirical observations from the Orange River, Republic of South Africa. Geomorphology 82, 160–172.
Stone, A., 2014. Last glacial maximum conditions in southern Africa: are we any closer to understanding the climate of this period? Prog. Phys. Geogr. 38 (5), 519–542.
Sugden, J.M., 1989. Palaeoecology of the Central and Marginal Uplands of the Karoo, South Africa. University of Cape Town, Cape Town, p. 384.
Temme, A., Baartman, J.E.M., Botha, G.A., Veldkamp, A., Jongmans, A.G., Wallinga, J., 2008. Climatic controls on late Pleistocene landscape evolution of the Okhombe valley, KwaZulu-Natal, South Africa. Geomorphology 99 (1–4), 280–295.
Tooth, S., McCarthy, T.S., Brandt, T., Hancox, P.J., Morris, R., 2002. Geological controls on the formation of alluvial meanders and floodplain wetlands: the example of the Klip River, eastern Free State, South Africa. Earth Surf. Process. Landf. 27 (8), 797–815.
Tooth, S., Brandt, D., Hancox, P.J., McCarthy, T.S., 2004. Geological controls on alluvial river behaviour: a comparative study of three rivers on the South African Highveld. J. Afr. Earth Sci. 38 (1), 79–97.
Tooth, S., Rodnight, H., Duller, G.A.T., McCarthy, T.S., Marren, P.M., Brandt, D., 2007. Chronology and controls of avulsion along a mixed bedrock-alluvial river. Geol. Soc. Am. Bull. 119 (3–4), 452–461.
Tooth, S., Hancox, P.J., Brandt, D., McCarthy, T.S., Jacobs, Z., Woodborne, S., 2013. Controls on the genesis, sedimentary architecture and preservation potential of dryland alluvial successions in stable continental interiors: insights from the incising Modder River, South Africa. J. Sediment. Res. 83, 541–561.
Trimble, S.W., 1983. A sediment budget for Coon Creek Basin in the Driftless Area, Wisconsin. J. Sci. 283, 454–474.
Tucker, G.E., Slingerland, R., 1997. Drainage basin responses to climate change. Water Resour. Res. 33 (8), 2031–2047.
Turner, B.R., 1978. Sedimentary patterns of uranium mineralisation in the Beaufort Group of the southern Karoo (Gondwana) Basin, South Africa. In: Miall, A.D. (Ed.), Fluvial Sedimentology. *Canadian Association of Petroleum Geologists*, Memoir 5, pp. 831–848.
Vandenberghe, J., 2003. Climate forcing of fluvial system development: an evolution of ideas. Quat. Sci. Rev. 22, 2053–2060.
Varnes, D.J., 1978. Slope movement types and processes. In: Schuster, R.L., Krizek, R.J. (Eds.), Landslides – Analysis and Control. National Research Council, Washington DC, Transportation Research Board, Special Report 176, pp. 11–33.
Verster, E., van Rooyen, T.H., 1999. Palaeosols on a fluvial terrace at Driekop, Northern Province, South Africa as indicators of climate change during the late Quaternary. Quat. Int. 57-58, 229–235.
Wang, Y., Straub, K.M., Hajek, E.A., 2011. Scale-dependent compensational stacking: an estimate of autogenic time scales in channelized sedimentary deposits. J. Geol. 39 (9), 811–814.
Wentworth, C.K., 1922. A scale of grade and class terms for clastic sediments. J. Geol. 30, 377–392.
Williams, M., 1992. Evidence for the dissolution of magnetite in recent Scottish peats. Quat. Res. 37 (2), 171–182.
Womack, W.R., Schumm, S.A., 1977. Terraces of Douglas Creek, northwestern Colorado: an example of episodic erosion. Geology 5 (2), 72–76.
Woodward, J.C., Hamlin, R.H.B., Macklin, M.G., Hughes, P.D., Lewin, J., 2008. Glacial activity and catchment dynamics in northwest Greece: long-term river behaviour and the slackwater sediment record for the last glacial to interglacial transition. Geomorphology 101, 44–67.
Wright, V.P., 1990. Estimating rates of calcrete formation and sediment accretion in ancient alluvial deposits. Geol. Mag. 127 (3), 273–276.
Wright, V.P., Platt, N.H., Wimbledon, W.A., 1988. Biogenic laminar calcretes: evidence of calcified root-mat horizons in palaeosols. Sedimentology 35 (4), 603–620.
Wright, V.P., Platt, N.H., Marriott, S.B., Beck, V.H., 1995. A classification of rhizogenic (root-formed) calcretes, with examples from the upper Jurassic-lower Cretaecous of Spain and upper cretaceous of southern France. Sediment. Geol. 100 (1–4), 143–158.
Yaalon, D.H., 1997. Soils in the Mediterranean region: what makes them different? Catena 28 (3–4), 157–169.
Young, R.W., Nanson, G.C., 1982. Terrace formation in the Illawarra region of new South Wales. Aust. Geogr. 15 (4), 212–219.
Zhang, P., Molnar, P., Downs, W., 2001. Increased sedimentation rates and grainsizes 2-4 Myr ago due to the influence of climate changes on erosion rates. Nature 410, 891–897.